LHC days in Split 2014

Event shapes methods for pp and p-Pb collisions

Antonio Ortiz Velasquez
Instituto de Ciencias Nucleares
Universidad Nacional Autónoma de México

September 30, 2014

Work in collaboration with:
Guy Paic and Eleazar Cuautle Flores

Plan for this talk

What are the event shapes?

Why are they interesting?

How can physics be extracted?

Where could this kind of analysis be implemented?

In the following, only results for transverse spherocity will be shown, but there are other variables: sphericity, thrust, aplanarity, circularity; which can be explored in the same way.

Event shapes at hadron colliders

- They provide a measurement of the energy flow in a hadron-hadron collision.
- They are restricted to the transverse plane in order to avoid the bias from the boost along the beam axis.
- By construction they are infrared and collinear safe.

A. Banfi, G. P. Salam and G. Zanderighi, JHEP 0408, 062, 2004.

- They can be used for MC tunning.

Example: Spherocity, S_O

$$S_O = \frac{\pi^2}{4} \min_{\vec{n}=(n_x,n_y,0)} \left(\frac{\sum |\vec{p}_{T_i} \times \vec{n}|}{\sum p_{T_i}} \right)^2$$

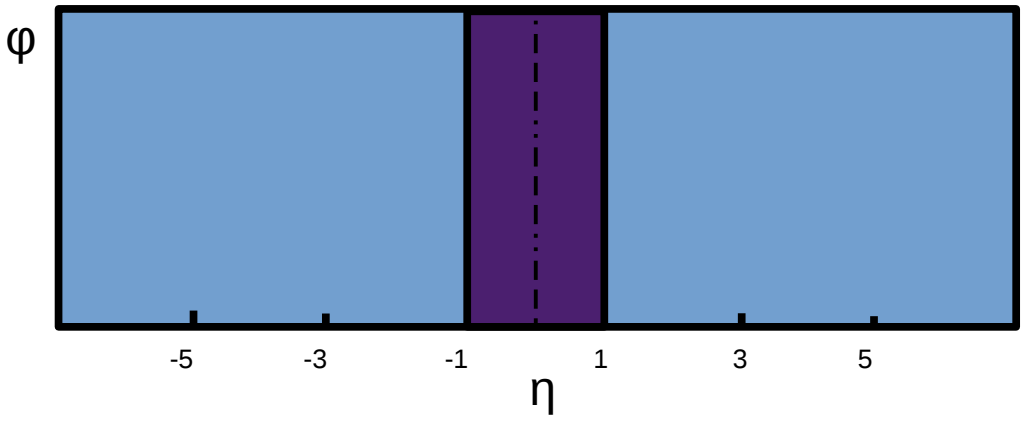

Defined for pp events having at least three primary charged hadrons within a given acceptance, $|\eta| < \eta_D$, and with transverse momentum above a threshold.

Spherocity close to zero.

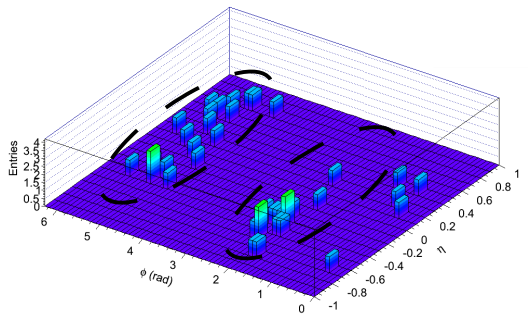

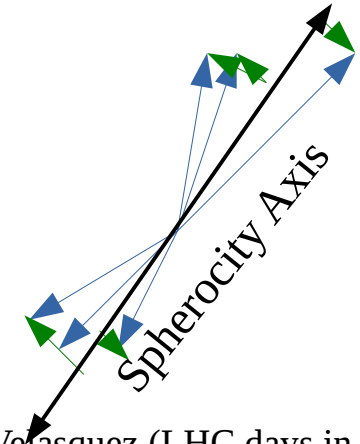

Spherocity close to one.

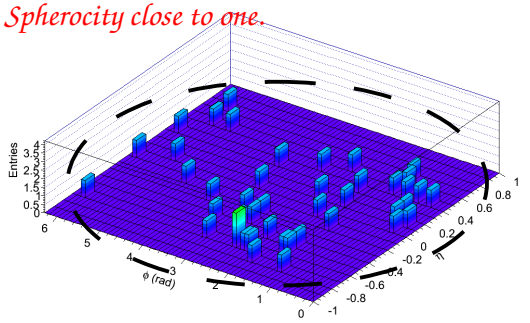

Example: Spherocity, S_O

$$S_O = \frac{\pi^2}{4} \min_{\vec{n}=(n_x, n_y, 0)} \left(\frac{\sum |\vec{p}_{T_i} \times \vec{n}|}{\sum p_{T_i}} \right)^2$$

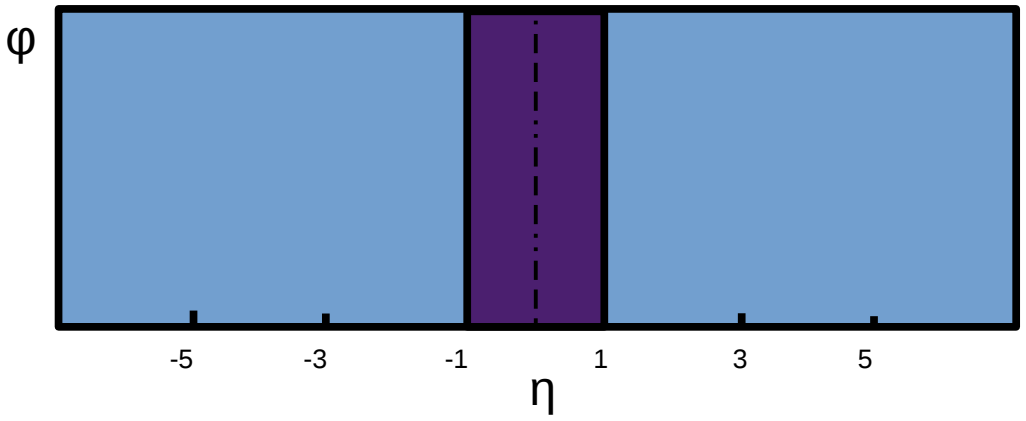

Defined for pp events having at least three primary charged hadrons within a given acceptance, $|\eta| < \eta_D$, and with transverse momentum above a threshold.

In this work we consider the following cuts:
$0.15 < p_T < 10$ GeV/c and $\eta_D = 1$
Motivated by different measurements reported by ALICE.

ALICE Collaboration, EPJC73: 2662 (2013), PLB727:371-380 (2013)

The results presented here were obtained using Pythia 8.180 tune 4C. This MC describes qualitatively well several observables measured at the LHC.

http://home.thep.lu.se/~torbjorn/Pythia.html

N_{ch} and Multi-parton interactions

Several semi-hard parton-parton scatterings may occur within the same pp collision, multi-parton interactions (MPI). This idea is supported by different measurements:

T. Akesson et al., Z. Phys. C 34, 163 (1987).
J. Alitti et al., Phys. Lett. B 268, 145 (1991).
F. Abe et al., Phys. Rev. D 56, 3811 (1997).

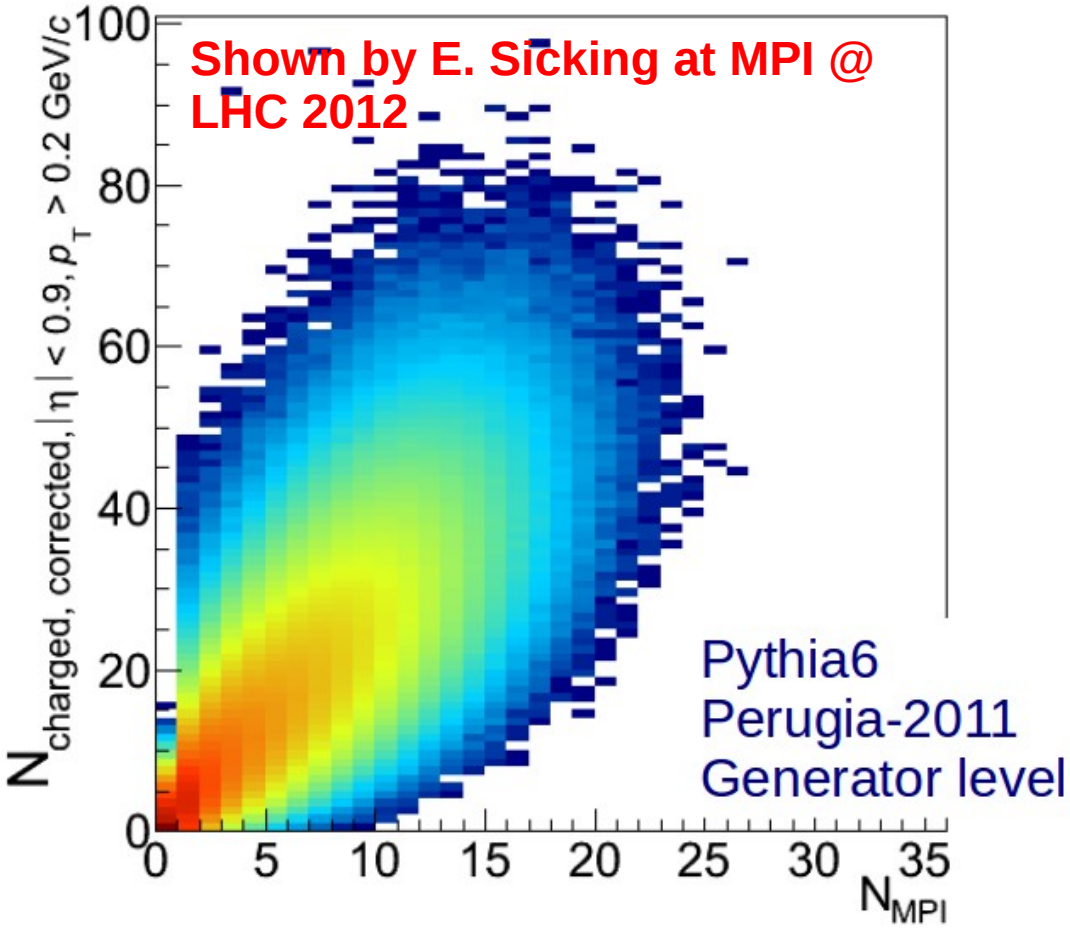

Multi-parton interactions are needed in Pythia for a good description of the hadron-hadron collisions data.

N_{ch} and Multi-parton interactions

Several semi-hard par
parton scatterings ma
occur within the same
collision, multi-parton
interactions (MPI). Thi
idea is supported by
different measuremen

T. Akesson et al., Z. Phys. C 34, 163 (1
J. Alitti et al., Phys. Lett. B 268, 145 (19
F. Abe et al., Phys. Rev. D 56, 3811 (19

Number of independent sources of particle production, in Pythia this is related with number of MPIs

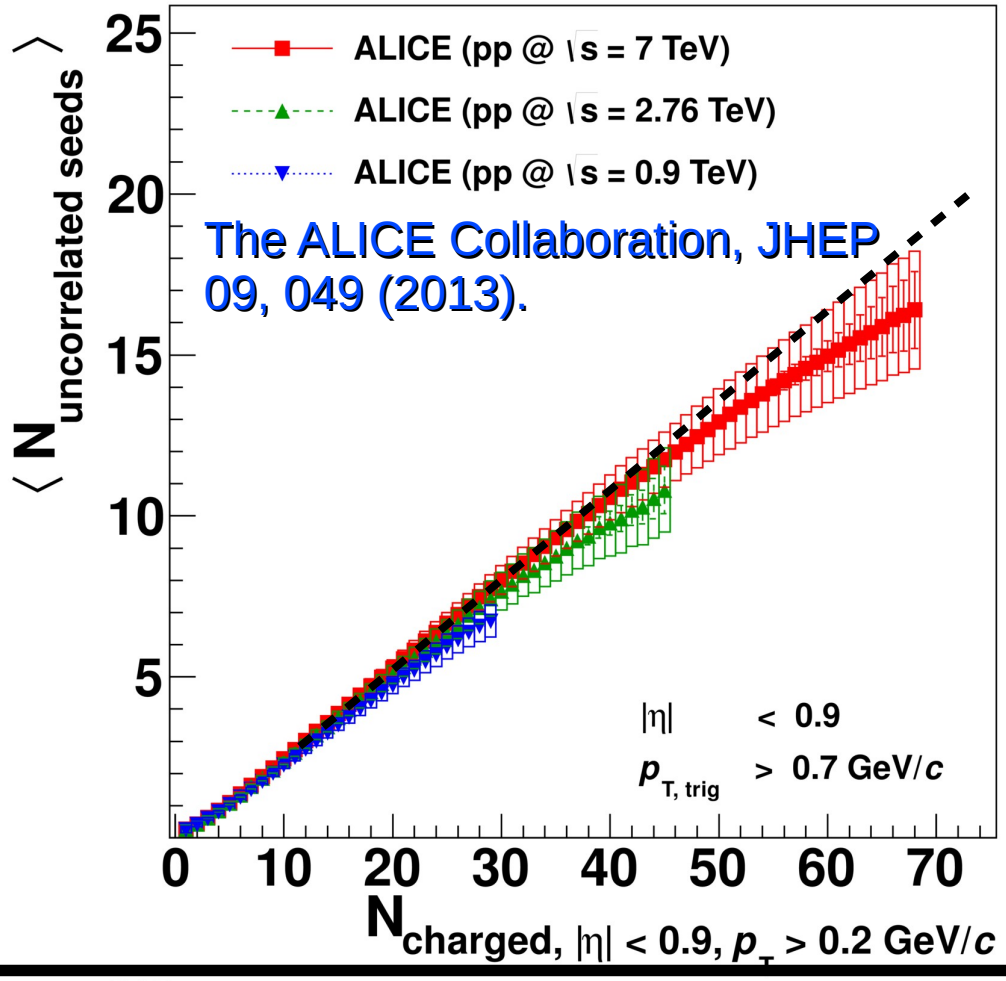

Multi-parton interactions ar
description of the hadron-hadron collisions data.

N_{ch} and Multi-parton interactions

Several semi-h
parton scatterin
occur within the
collision, multi-p
interactions (MI
idea is supporte
different measu

T. Akesson et al., Z. Phys. C
J. Alitti et al., Phys. Lett. B
F. Abe et al., Phys. Rev. D

Multi-parton interac
description of the h

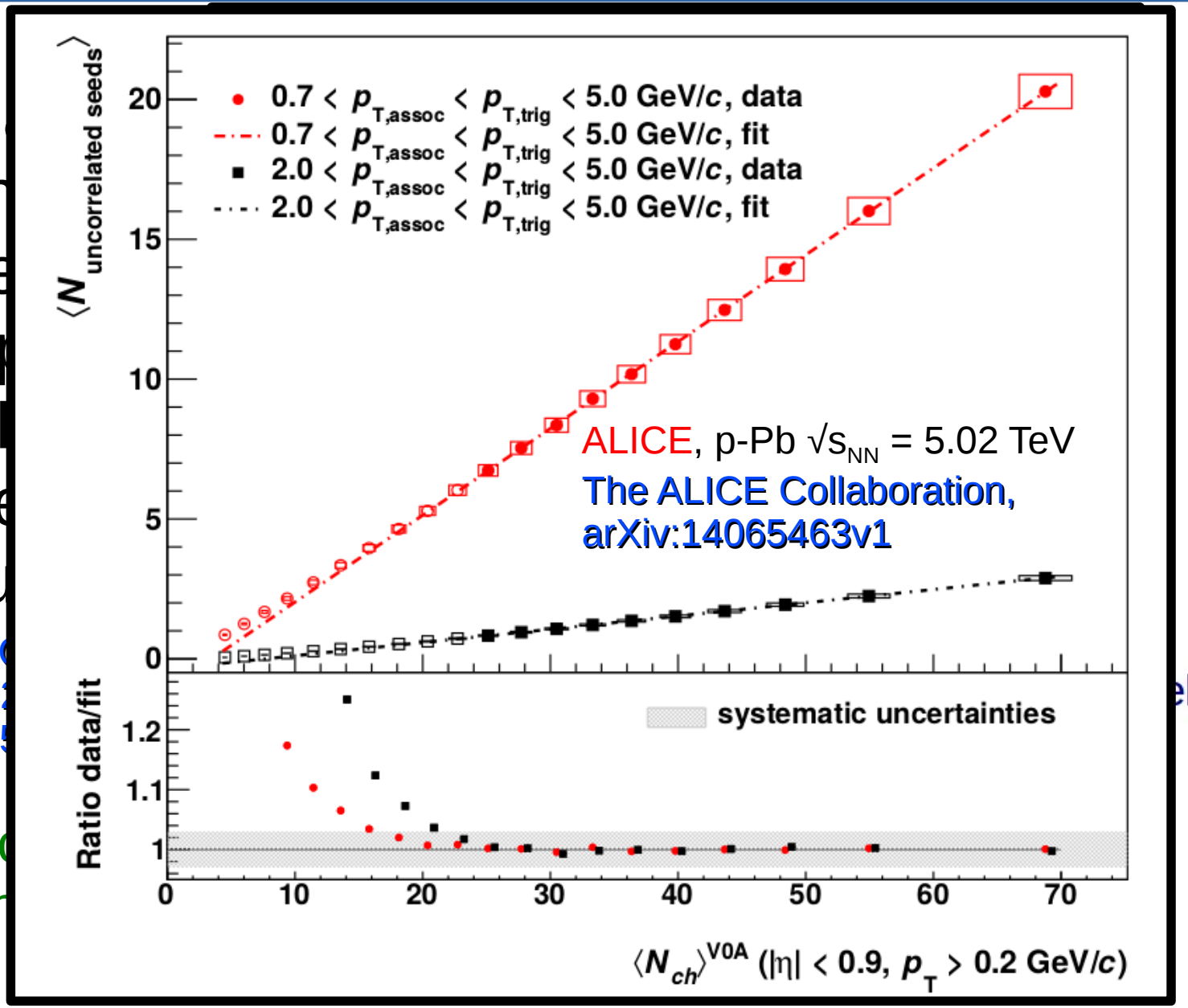

N_{ch}, S_O (|η|<1) and MPI

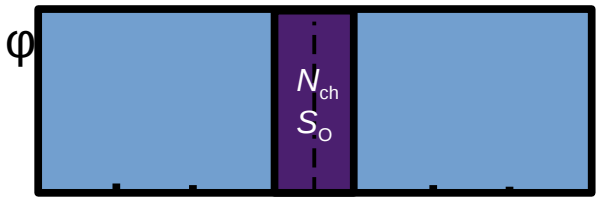

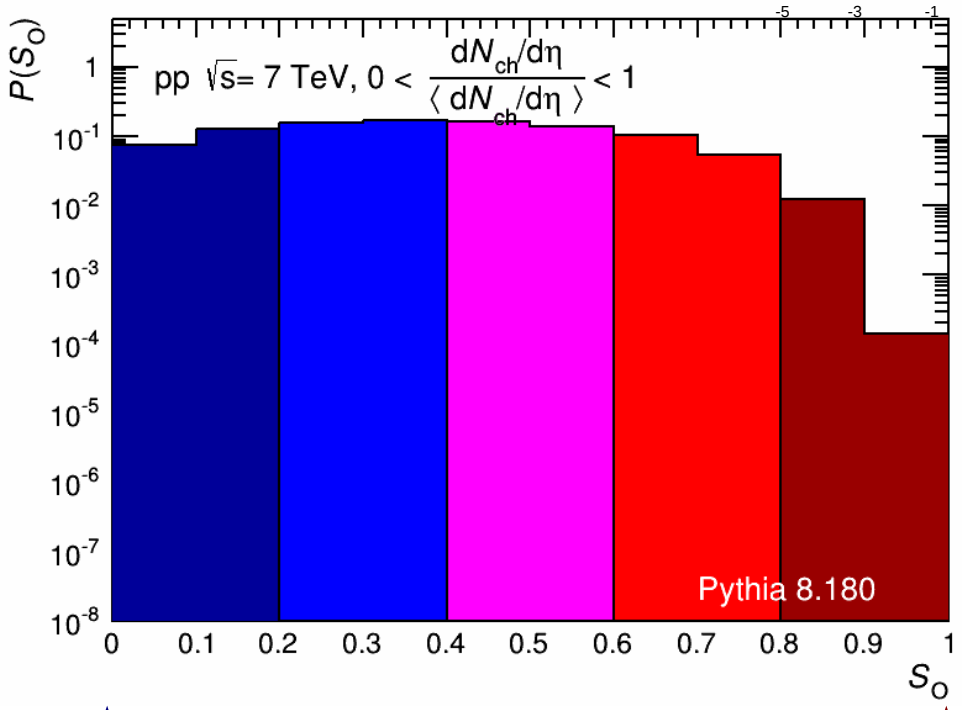

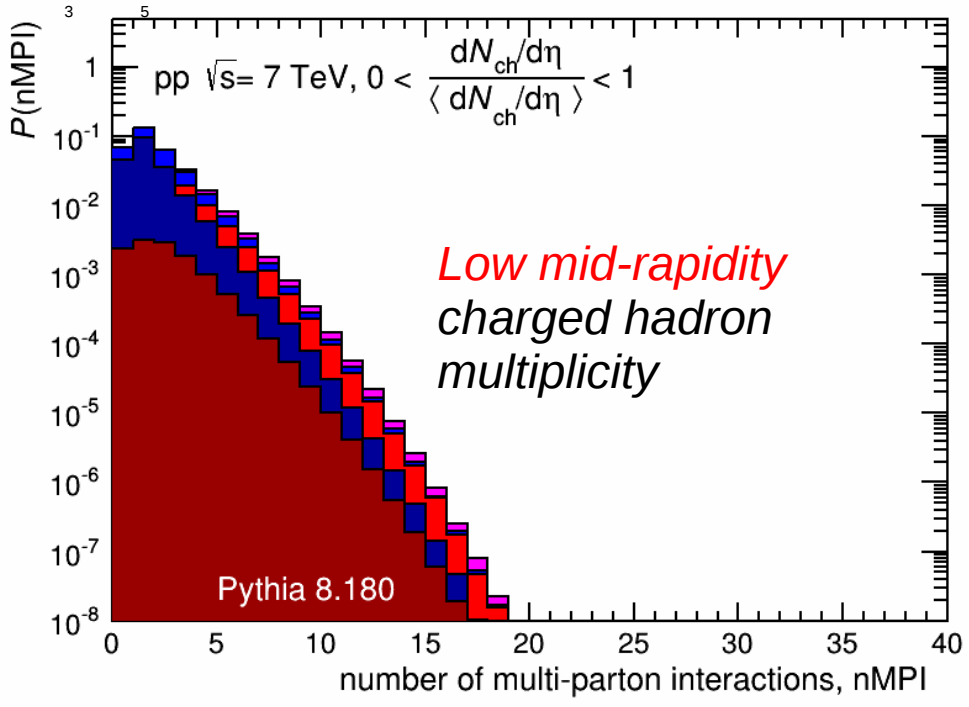

Low mid-rapidity charged hadron multiplicity

Pencil-like limit

Isotropic limit

E. Cuautle et. al., arXiv:1404.2372

N_{ch}, S_O (|η|<1) and MPI

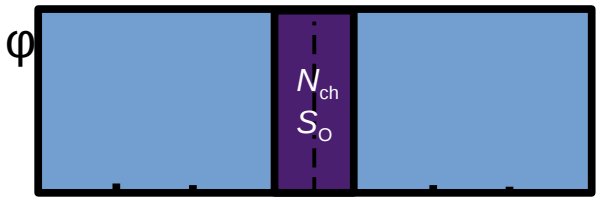

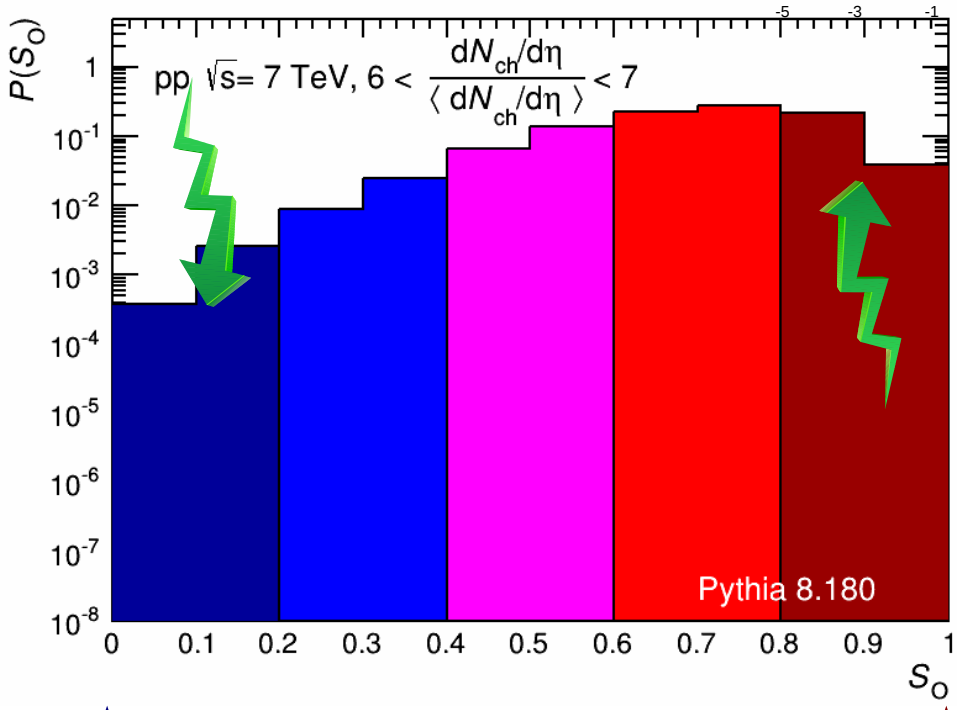

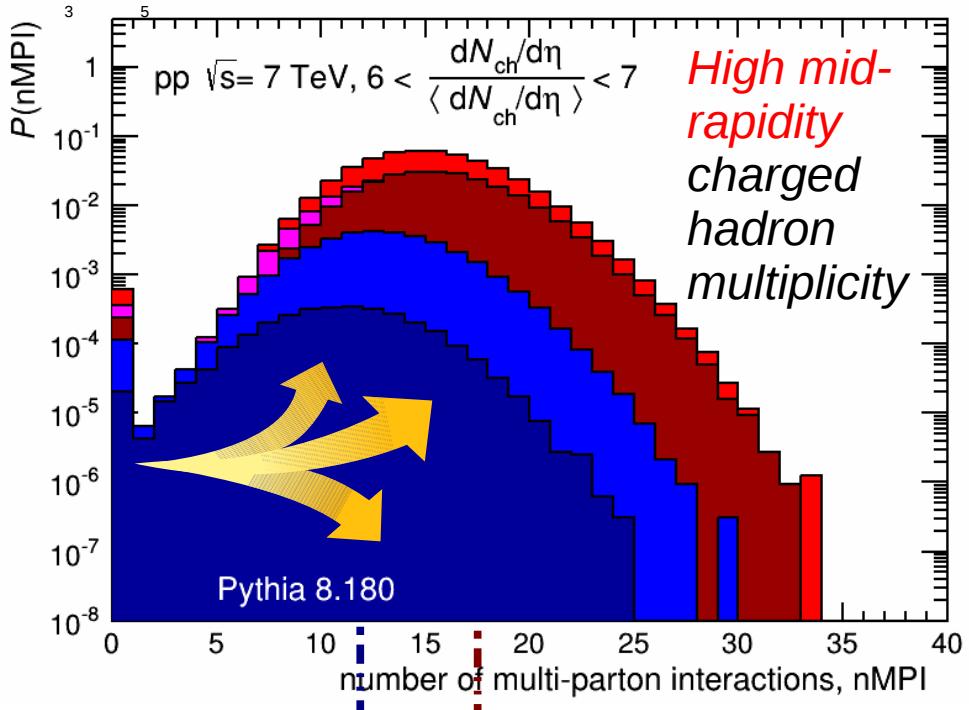

Pencil-like limit

Isotropic limit

E. Cuautle et. al., arXiv:1404.2372

Jet production vs N_{ch} and S_O

Fast jet 3.0.6

M. Cacciari, G.P. Salam and G. Soyez, EPJC72, 1896, 2012.

- Anti-k_T algorithm.
- Jet size, R = 0.4
- **Min p_T jet: 10 GeV/c**
- Only charged constituents.

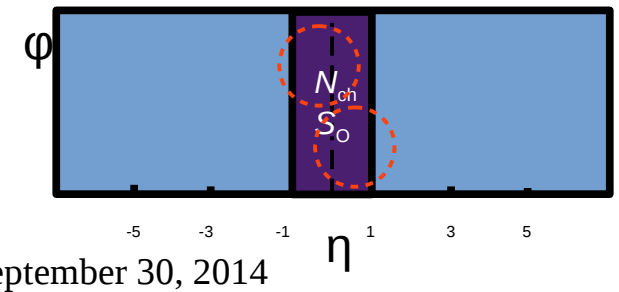

Average number of jets vs multiplicity

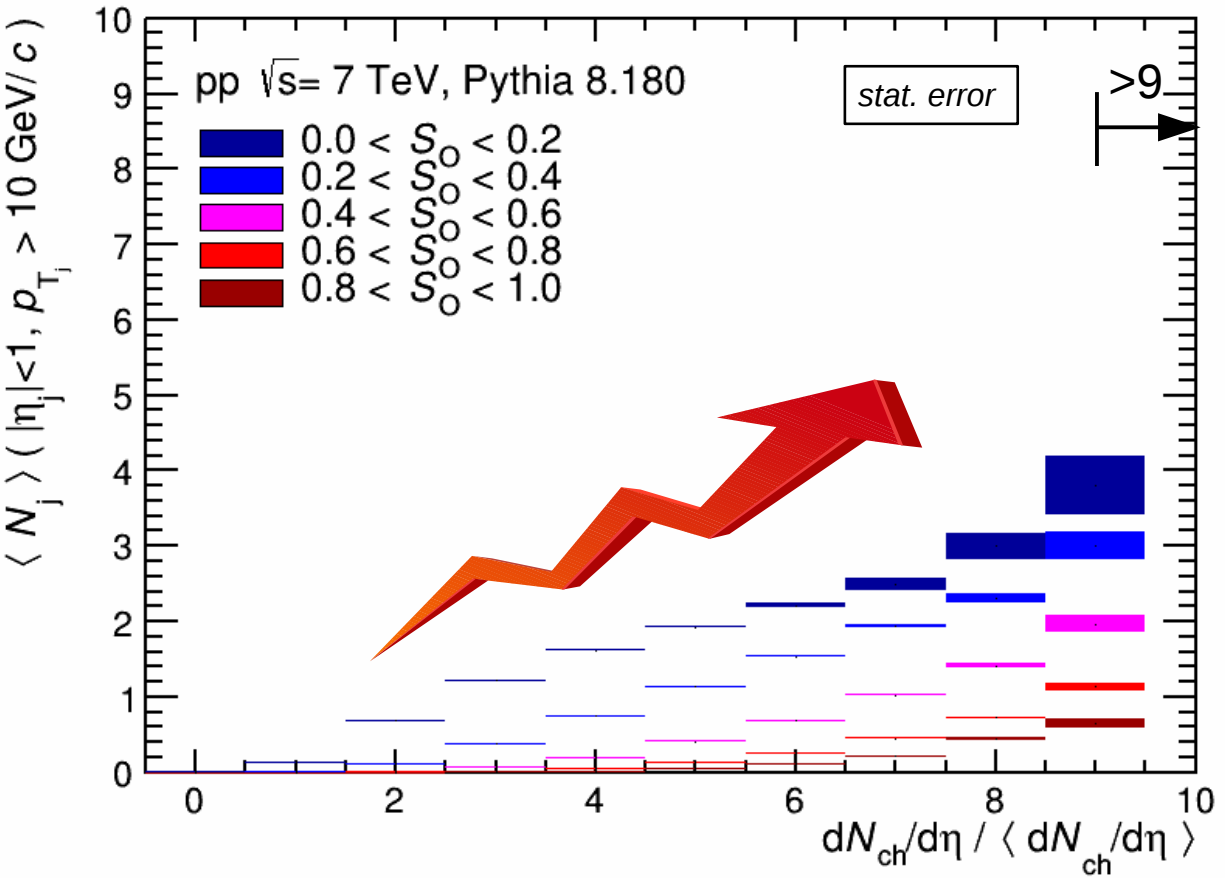

(Jet multiplicity distributions are shown in the backup)

*The inclusive case (w/o any cut on S_O) roughly follows the magenta points

Jet-p_T vs N_{ch} and S_O

Fast jet 3.0.6

M. Cacciari, G.P. Salam and G. Soyez, EPJC72, 1896, 2012.

- Anti-k_T algorithm.
- Jet size, R = 0.4
- **Min p_T jet: 10 GeV/c**
- Only charged constituents.

Average jet p_T vs multiplicity

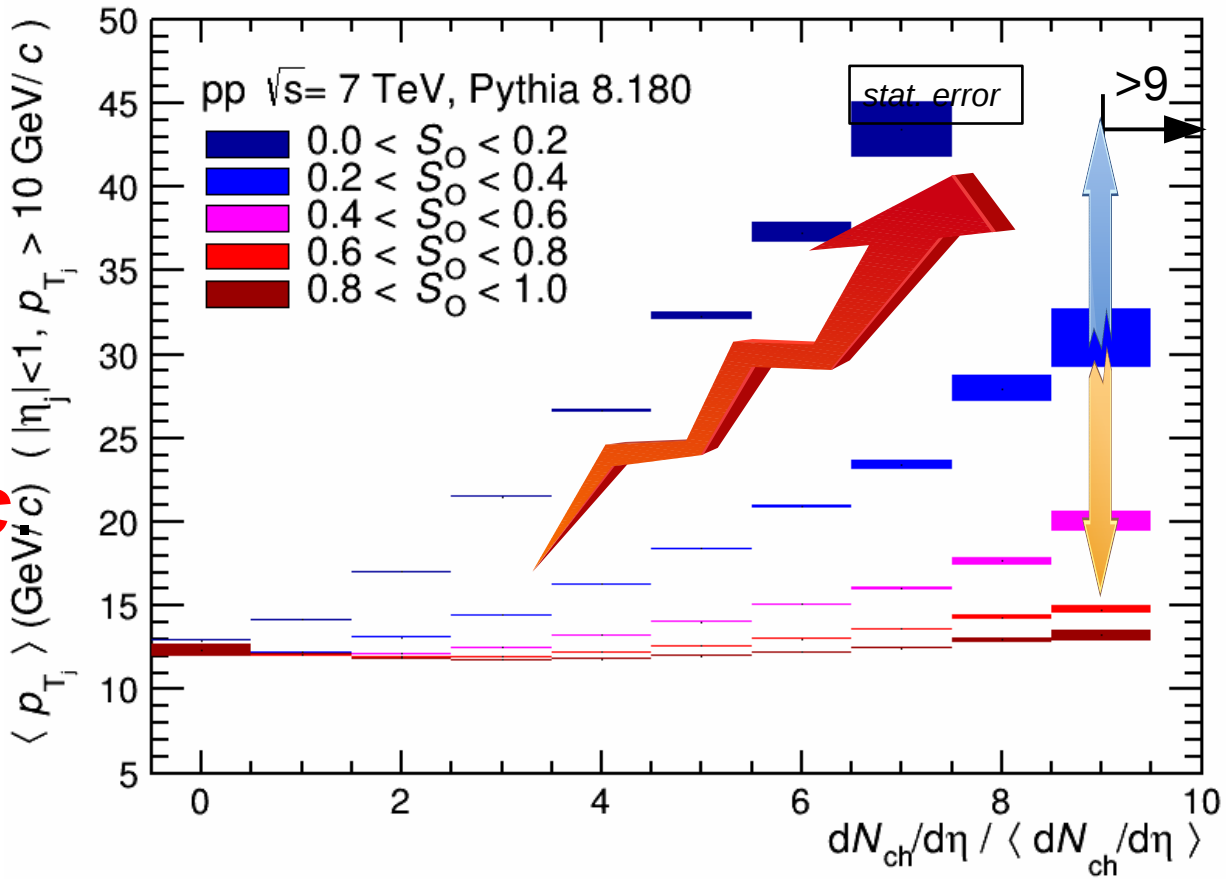

(Jet transverse momentum distributions are shown in the backup)

*The inclusive case (w/o any cut on S_O) roughly follows the magenta points

Jet-p_T vs N_{ch} and S_O

Fast jet 3.0.6

M. Cacciari, G.P. Salam and G. Soyez, EPJC72, 1896, 2012.

The analysis in a small acceptance allows the identification of events with pure underlying event (high S_O), or high p_T jets (low S_O).

In the experiments what we have done so far, is to study averages. But, the event shape approach is ideal for more detailed studies of the pp interactions.

Average jet p_T vs multiplicity

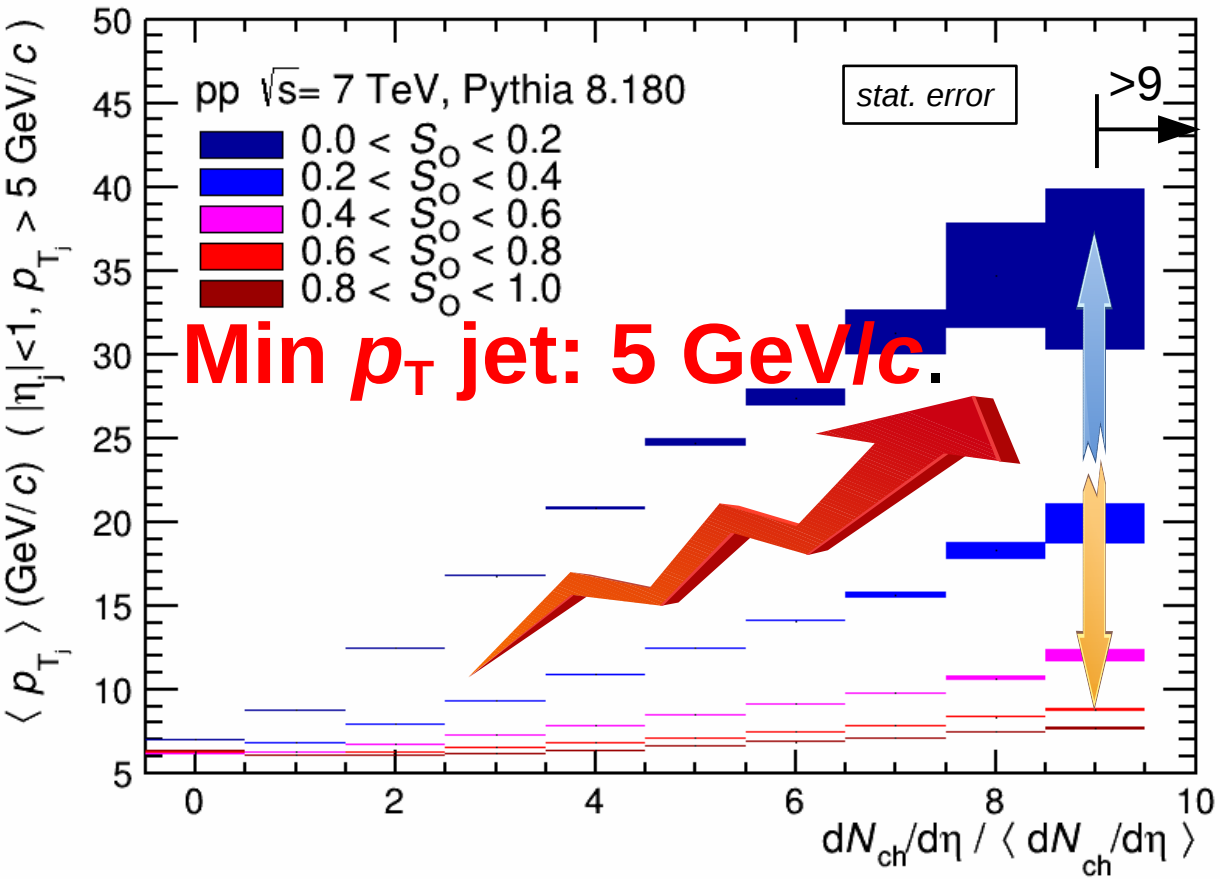

(Jet transverse momentum distributions are shown in the backup)

*The inclusive case (w/o any cut on S_O) roughly follows the magenta points

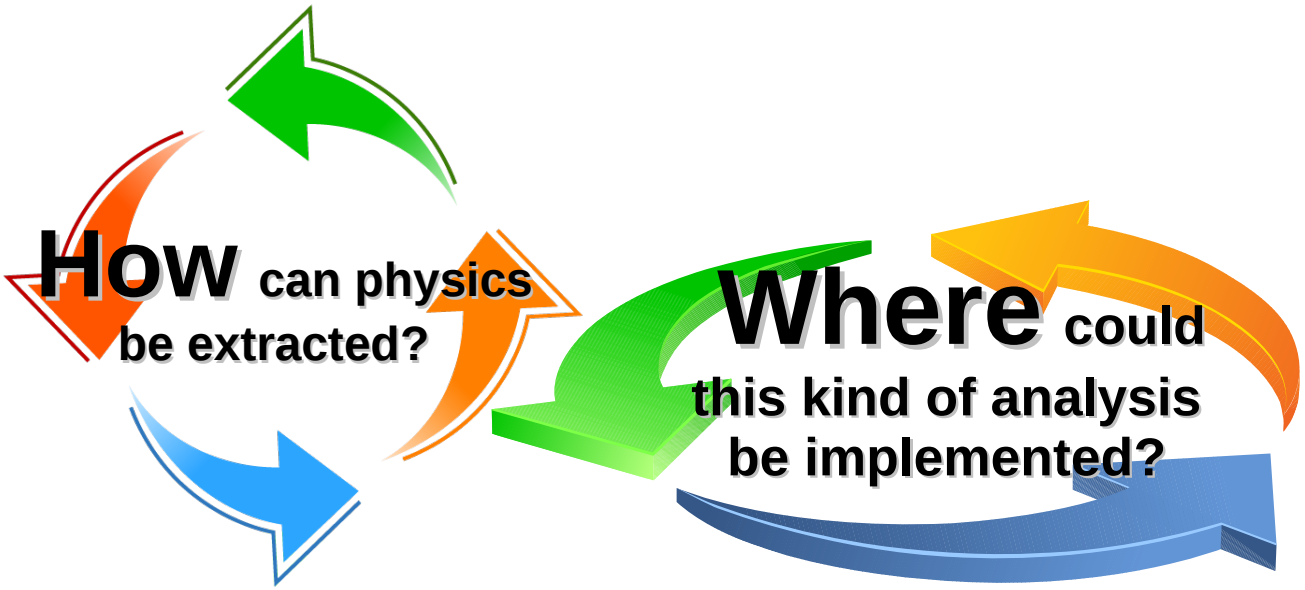

The following slides show results where all the observables (p_T spectra, spherocity and multiplicity) are calculated using hadrons within the same acceptance, $|\eta|<1$. Results when N_{ch} is obtained at forward pseudorapidity are shown in the backup.

<p_T> vs N_{ch} for charged hadrons

A similar effect is observed when one considers inclusive charged hadrons.

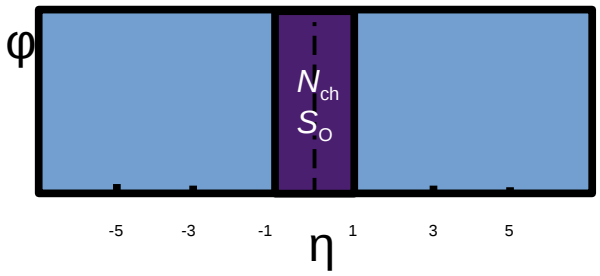

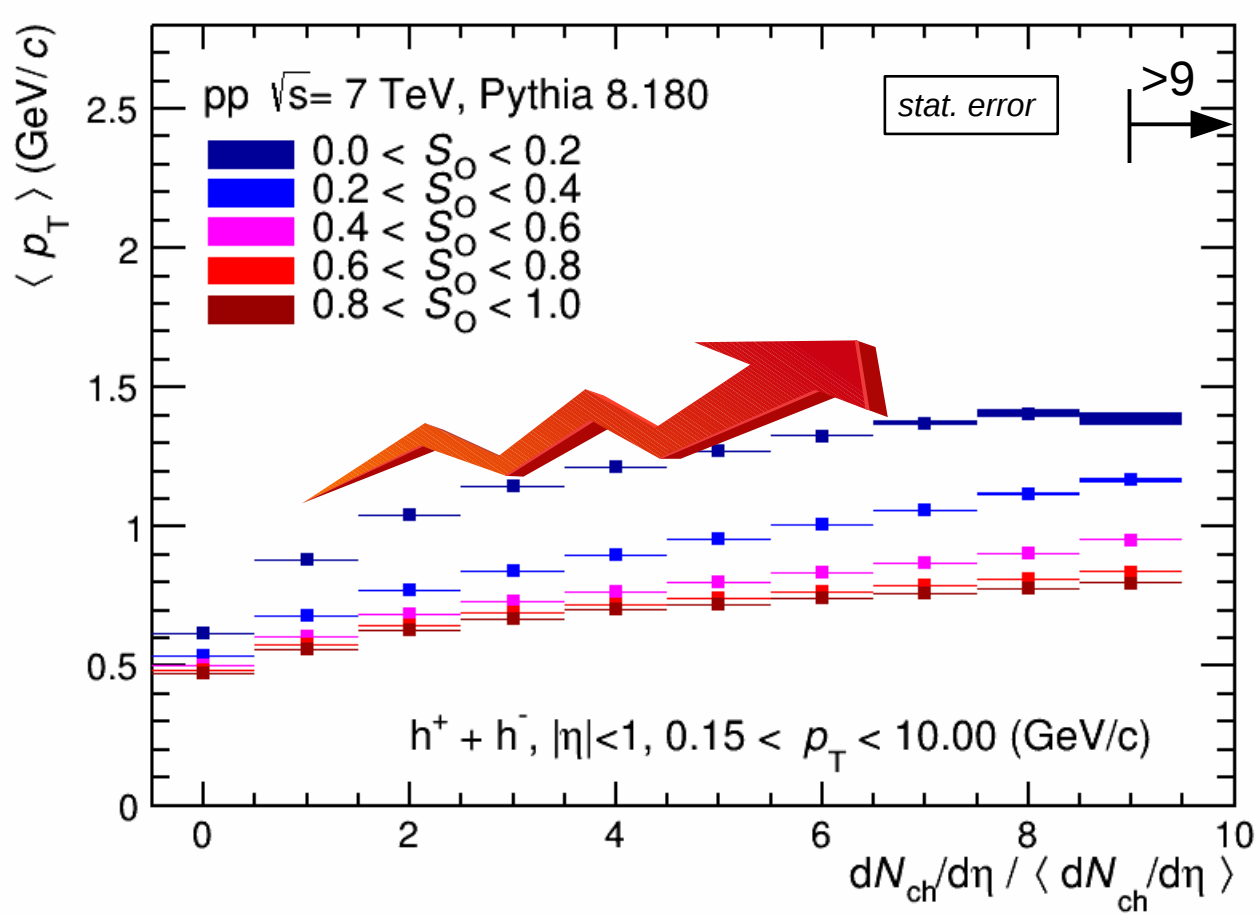

*The inclusive case (w/o any cut on S_O) roughly follows the magenta points

$\langle p_T \rangle$ vs N_{ch} for charged hadrons

A similar effect is observed when one considers inclusive charged hadrons.

At high N_{ch}:
A second rise of the mean p_T is observed when S_O<0.6 (more jetty-like).

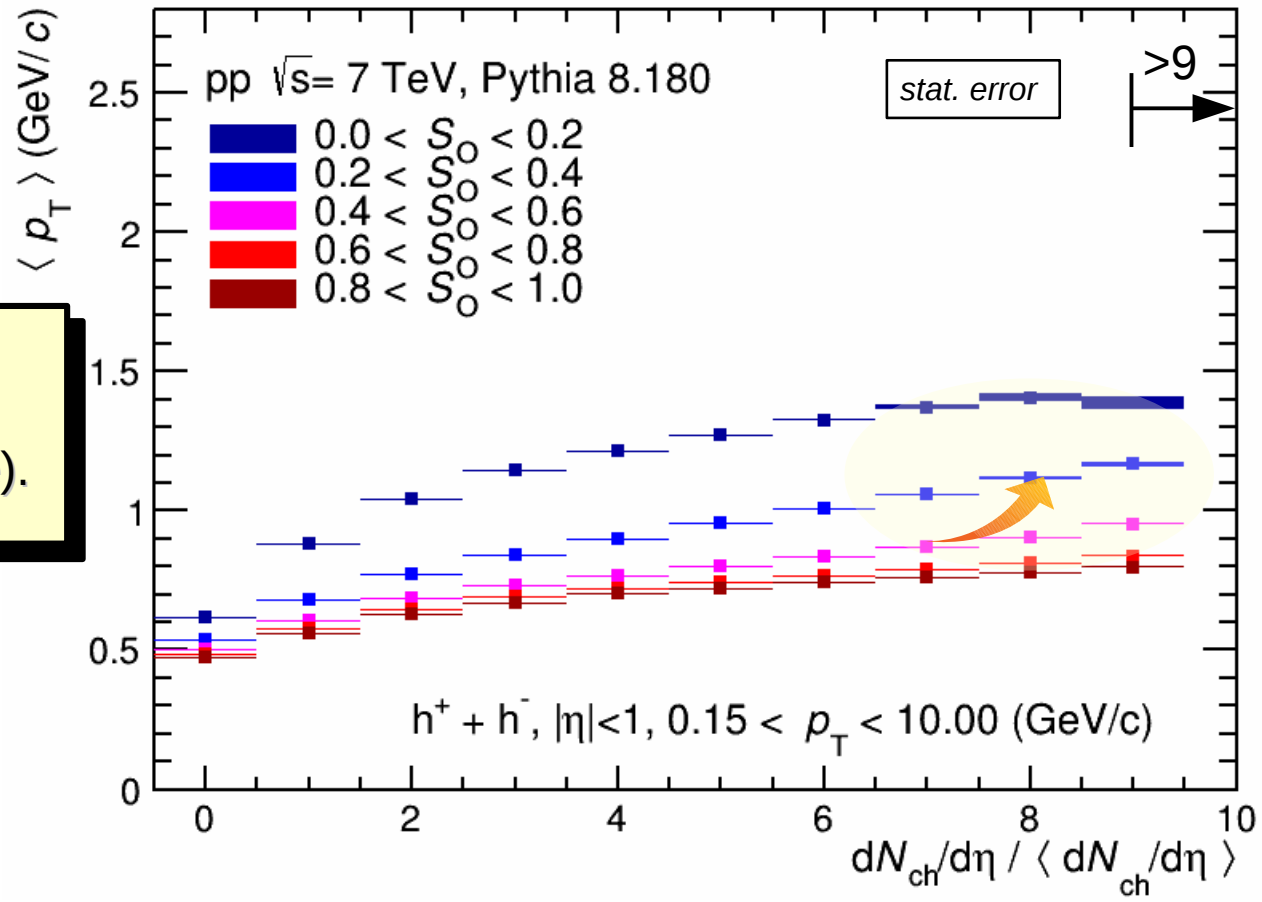

*The inclusive case (w/o any cut on S_O) roughly follows the magenta points

$\langle p_T \rangle$ vs N_{ch} for charged hadrons

A similar effect is observed when one considers inclusive charged hadrons.

At high N_{ch}:
A second rise of the mean p_T is observed when S_O<0.6 (more jetty-like).

The effect is smaller in isotropic events.

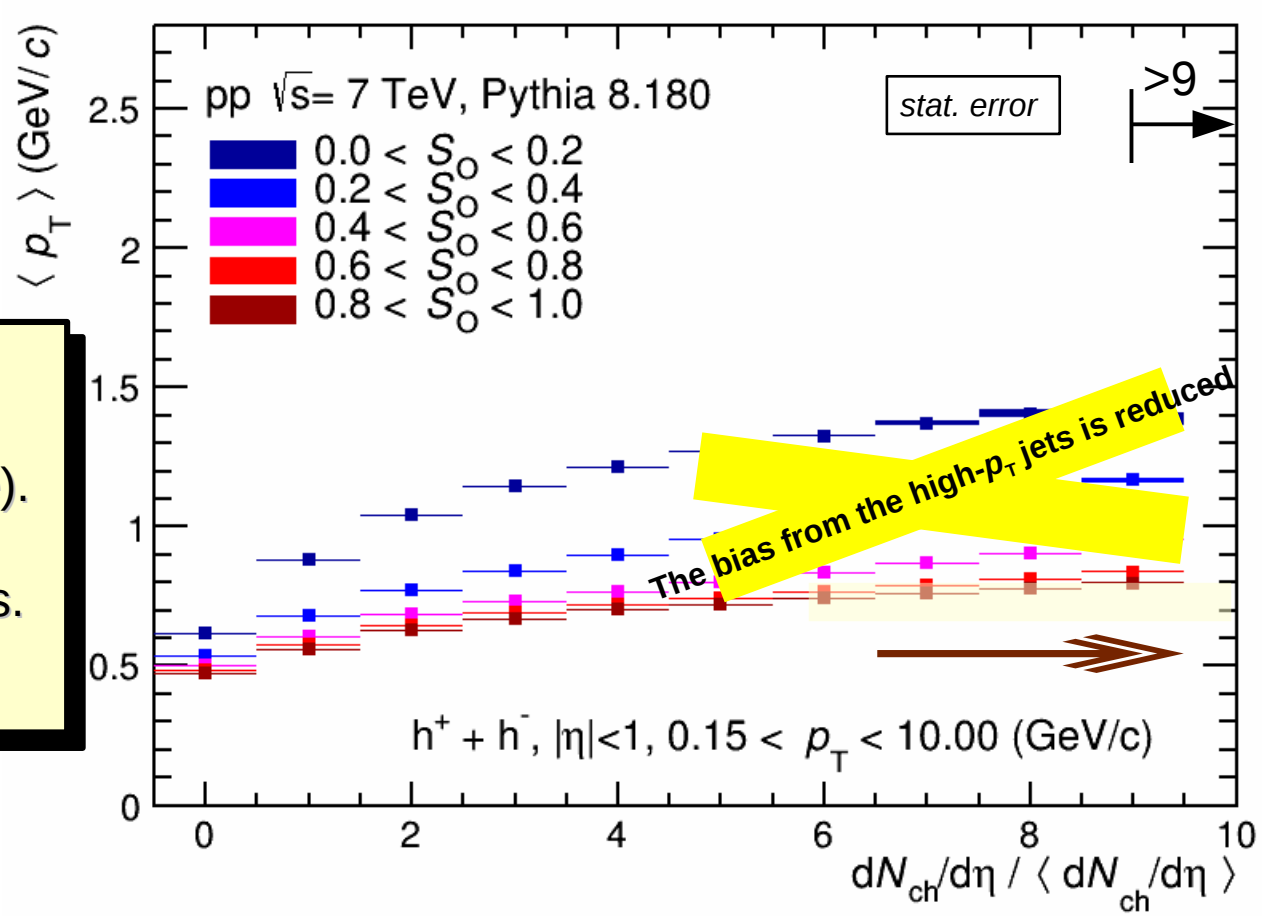

*The inclusive case (w/o any cut on S_O) roughly follows the magenta points

<p_T> vs N_{ch} for charged hadrons

A similar effect is observed when one considers inclusive charged hadrons.

At high N_{ch}:
A second rise of the mean p_T is observed when S_O<0.6 (more jetty-like).

The effect is smaller in isotropic events .

<p_T> in p-Pb collisions is flatter than the one measured in pp collisions. Is this an effect of MPIs? ALICE Collaboration, PLB727:371-380 (2013).

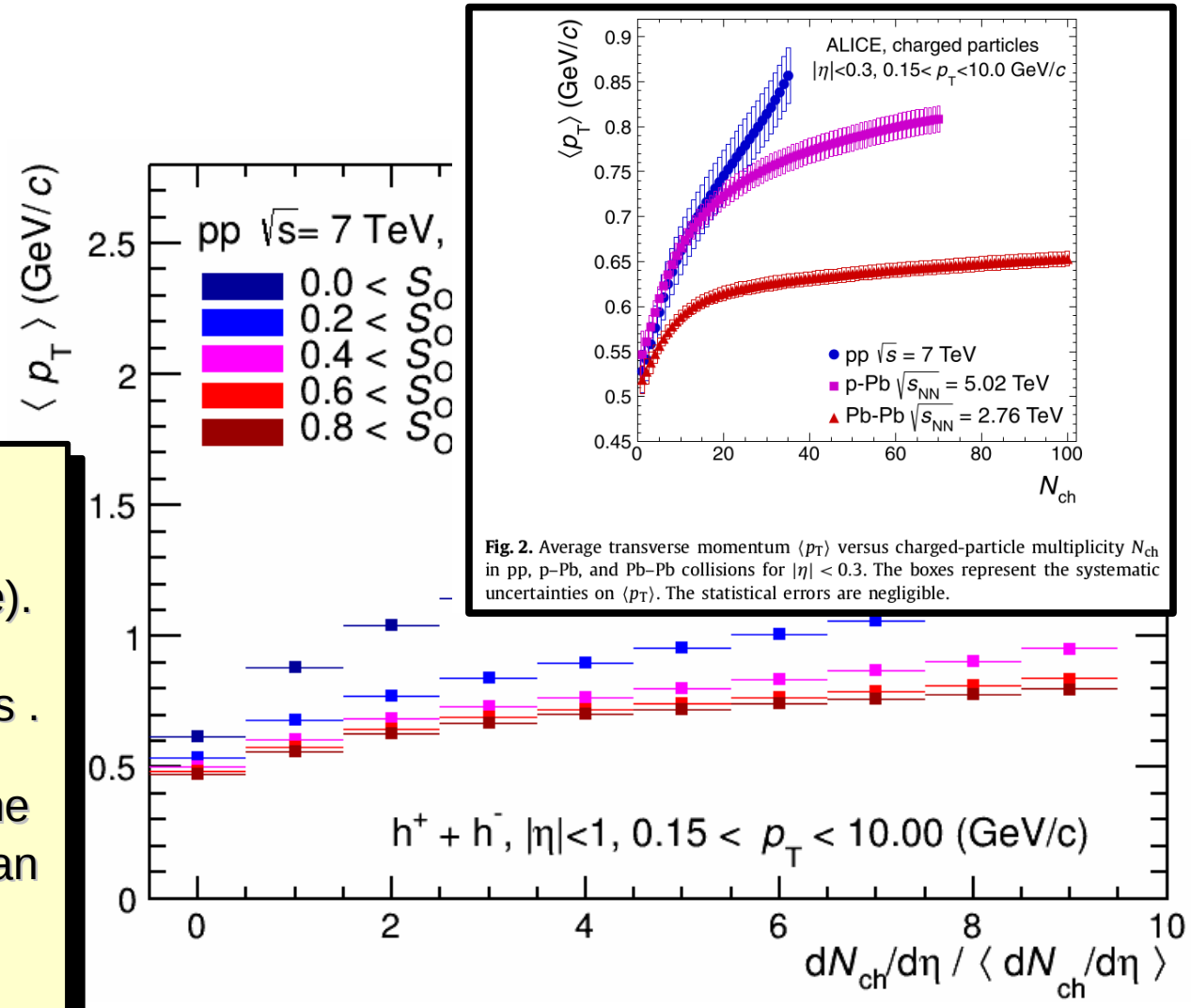

Fig. 2. Average transverse momentum $\langle p_T \rangle$ versus charged-particle multiplicity N_{ch} in pp, p–Pb, and Pb–Pb collisions for $|\eta| < 0.3$. The boxes represent the systematic uncertainties on $\langle p_T \rangle$. The statistical errors are negligible.

Particle ratios vs p_T

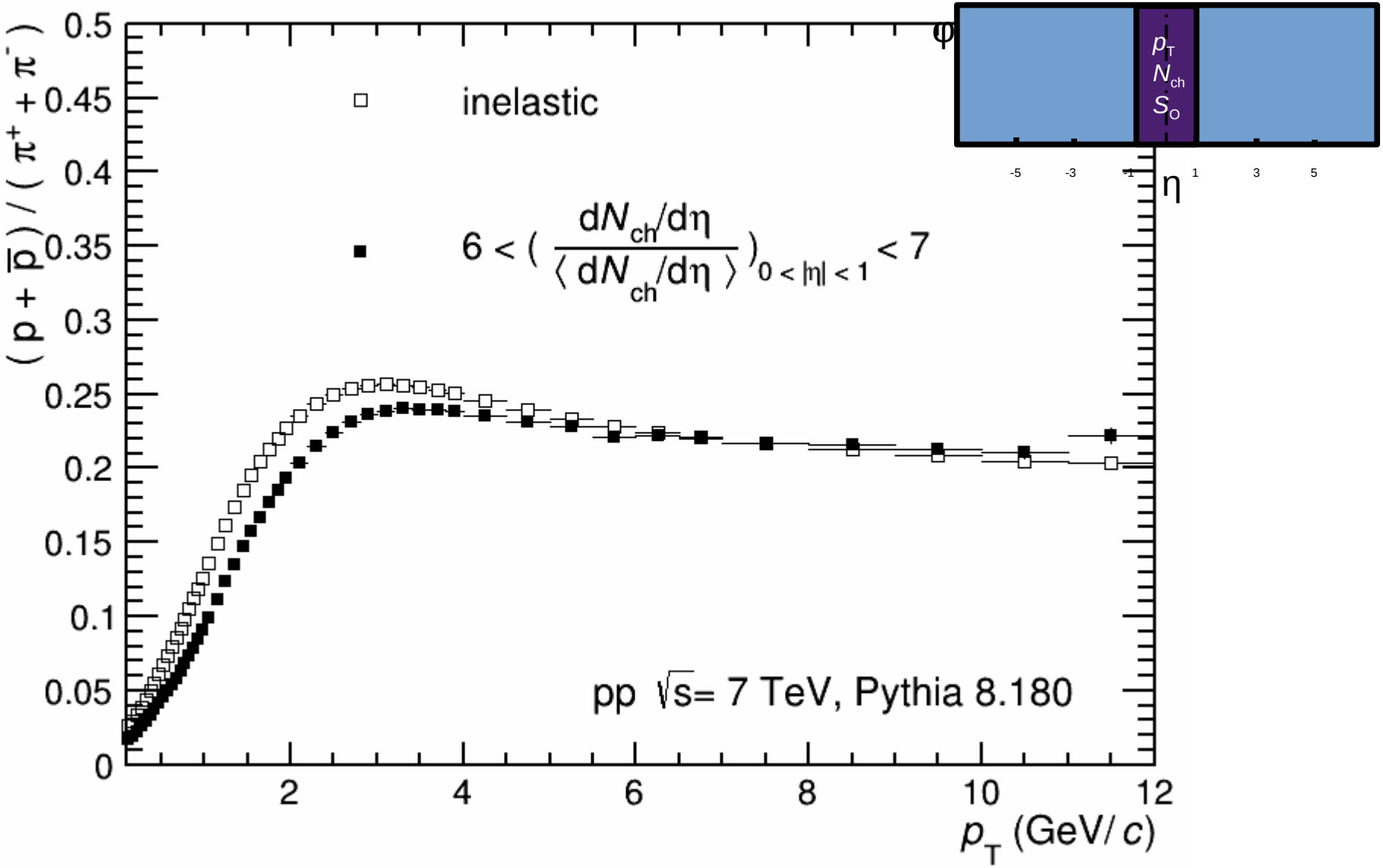

Particle ratios vs p_T

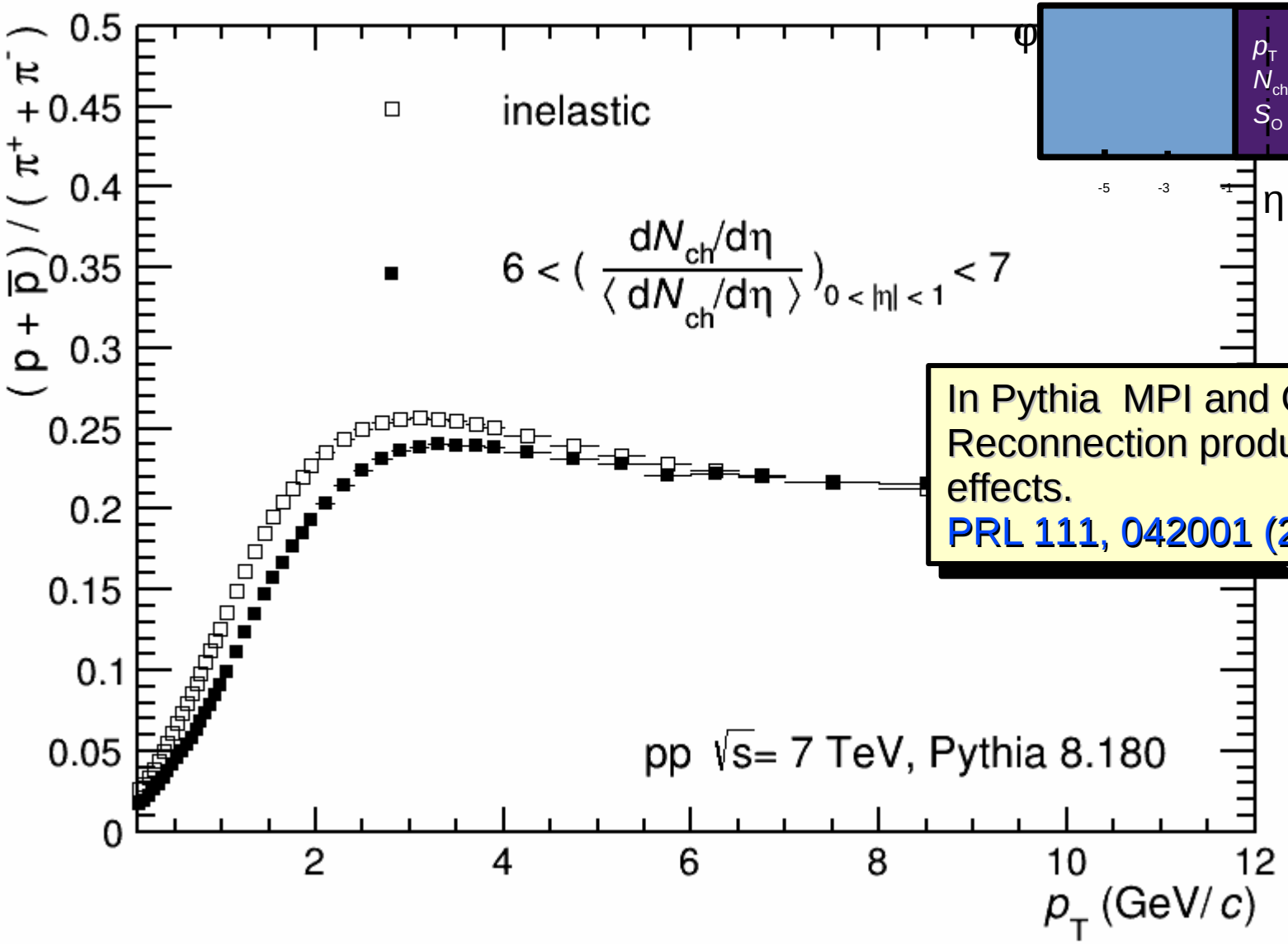

In Pythia MPI and Color Reconnection produce flow-like effects.
PRL 111, 042001 (2013).

Particle ratios vs p_T

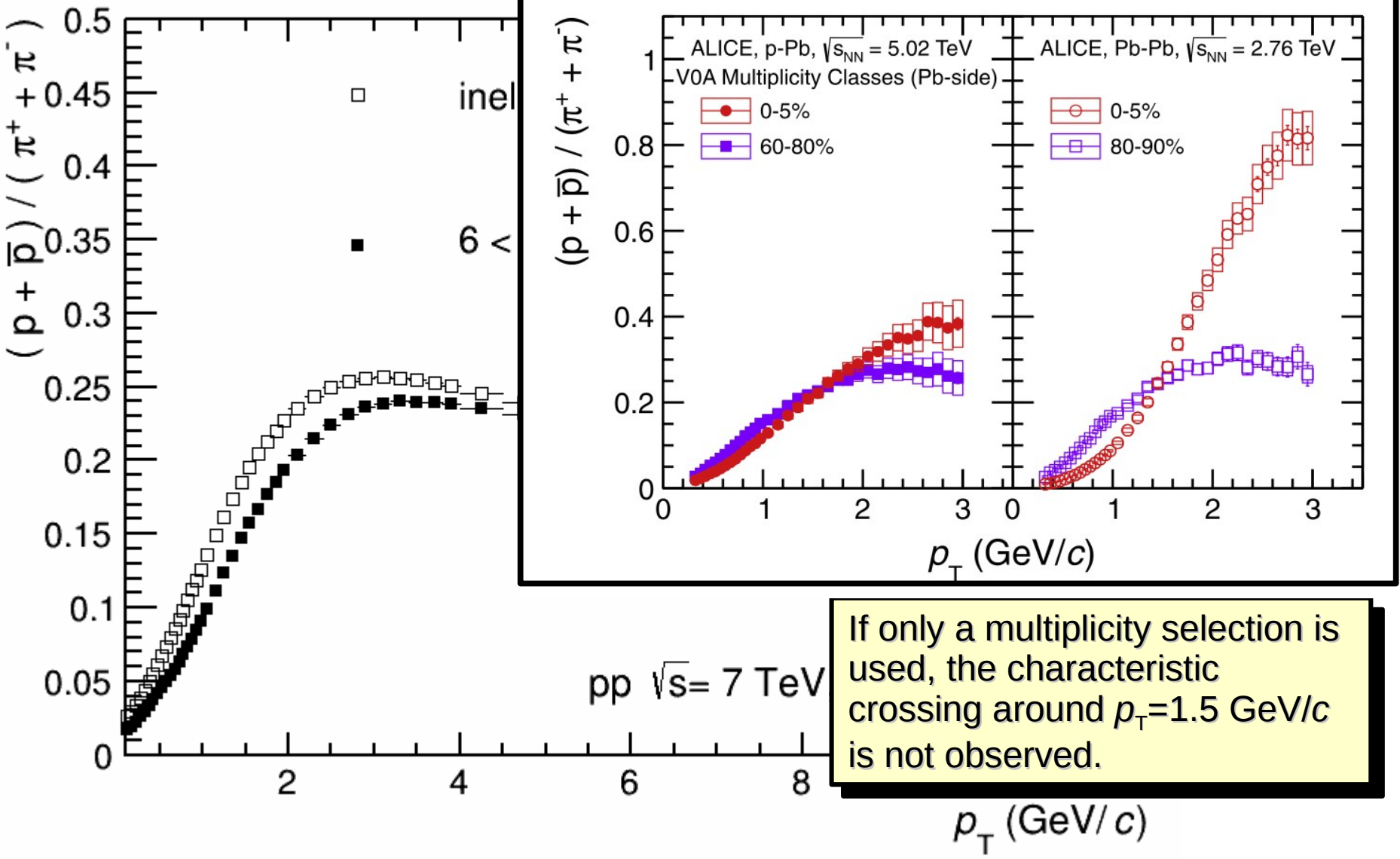

If only a multiplicity selection is used, the characteristic crossing around p_T=1.5 GeV/c is not observed.

Particle ratios vs p_T

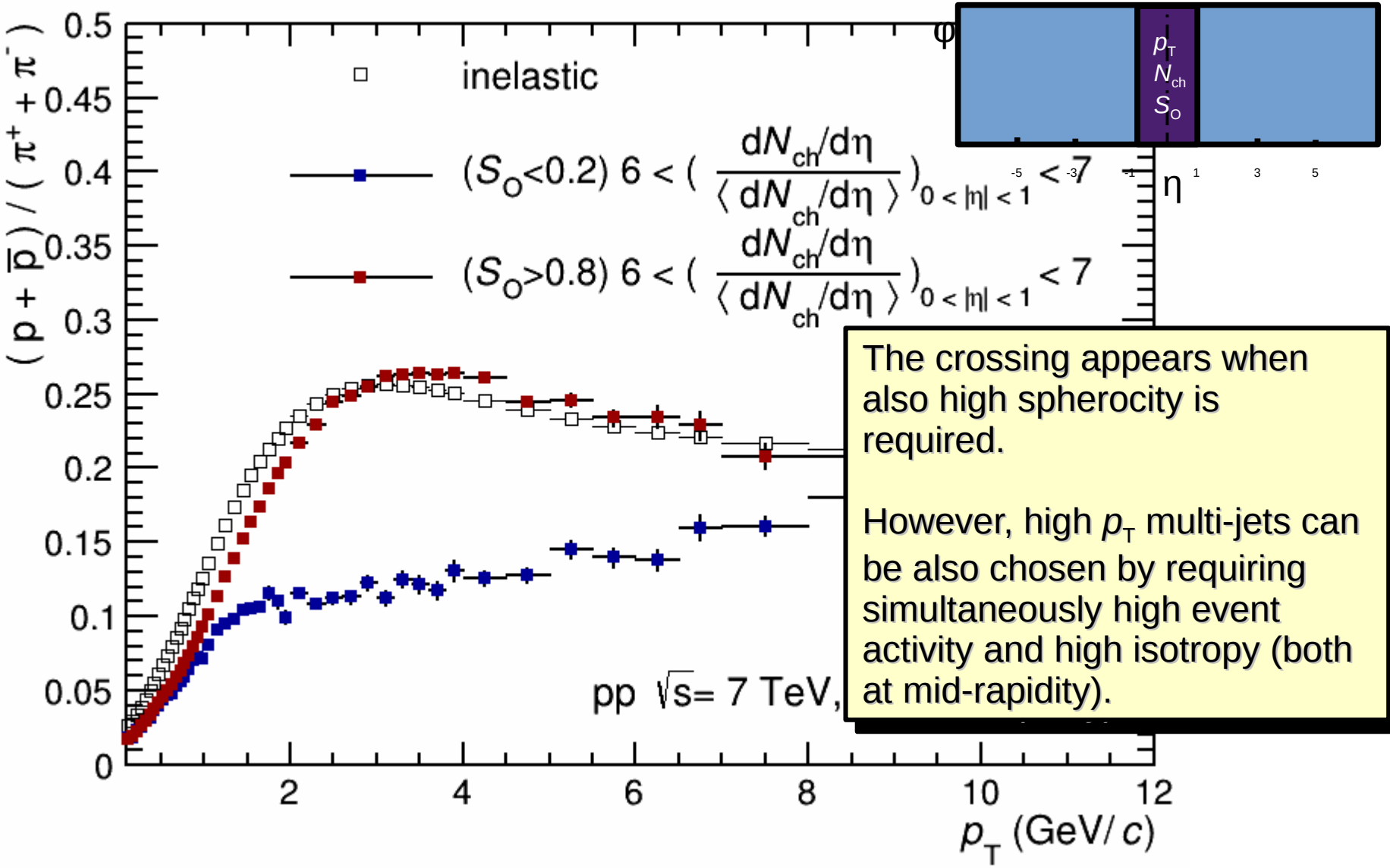

The crossing appears when also high spherocity is required.

However, high p_T multi-jets can be also chosen by requiring simultaneously high event activity and high isotropy (both at mid-rapidity).

Particle ratios vs p_T

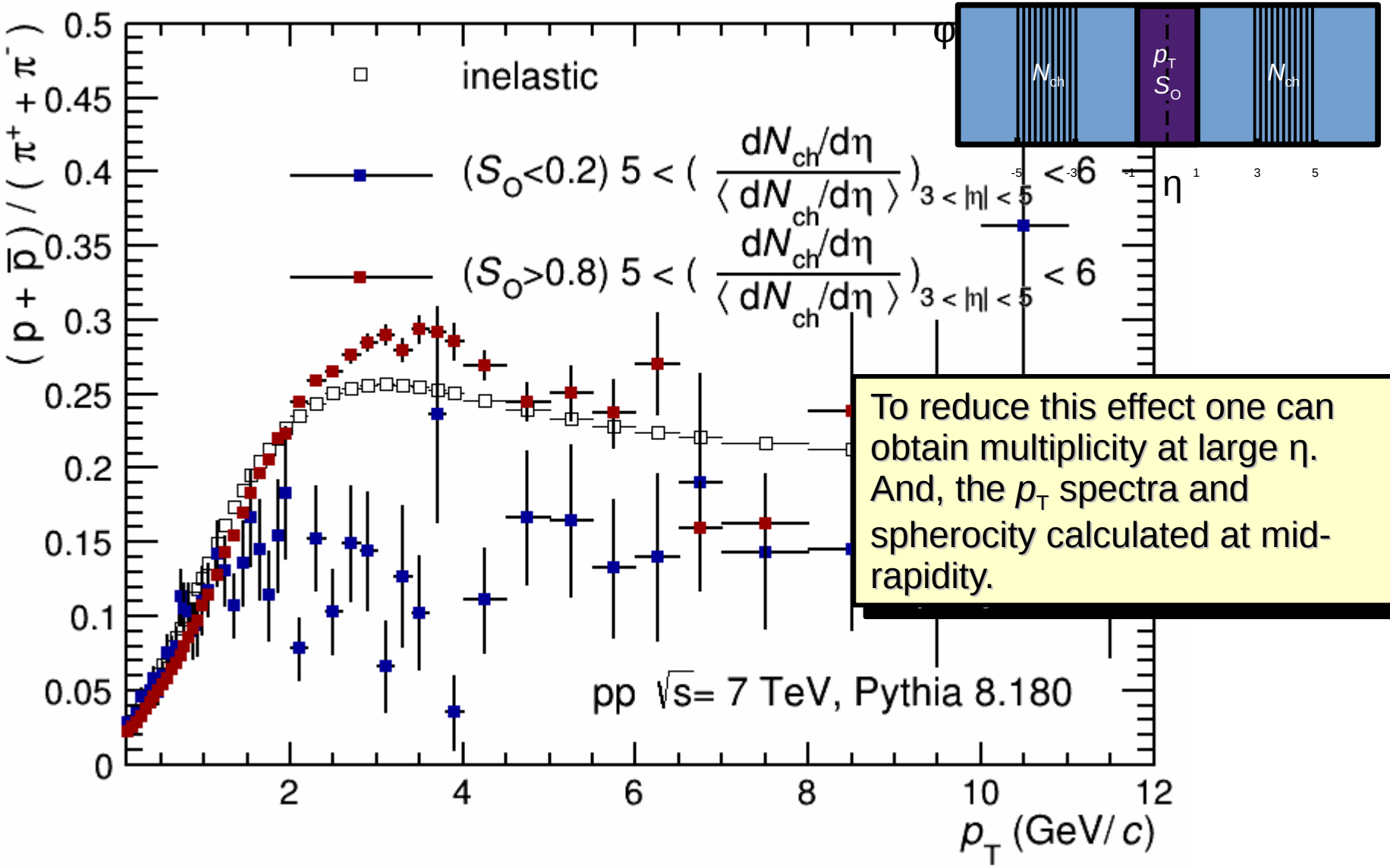

To reduce this effect one can obtain multiplicity at large η. And, the p_T spectra and spherocity calculated at mid-rapidity.

Mass ordering

High mid-rapidity charged hadron multiplicity

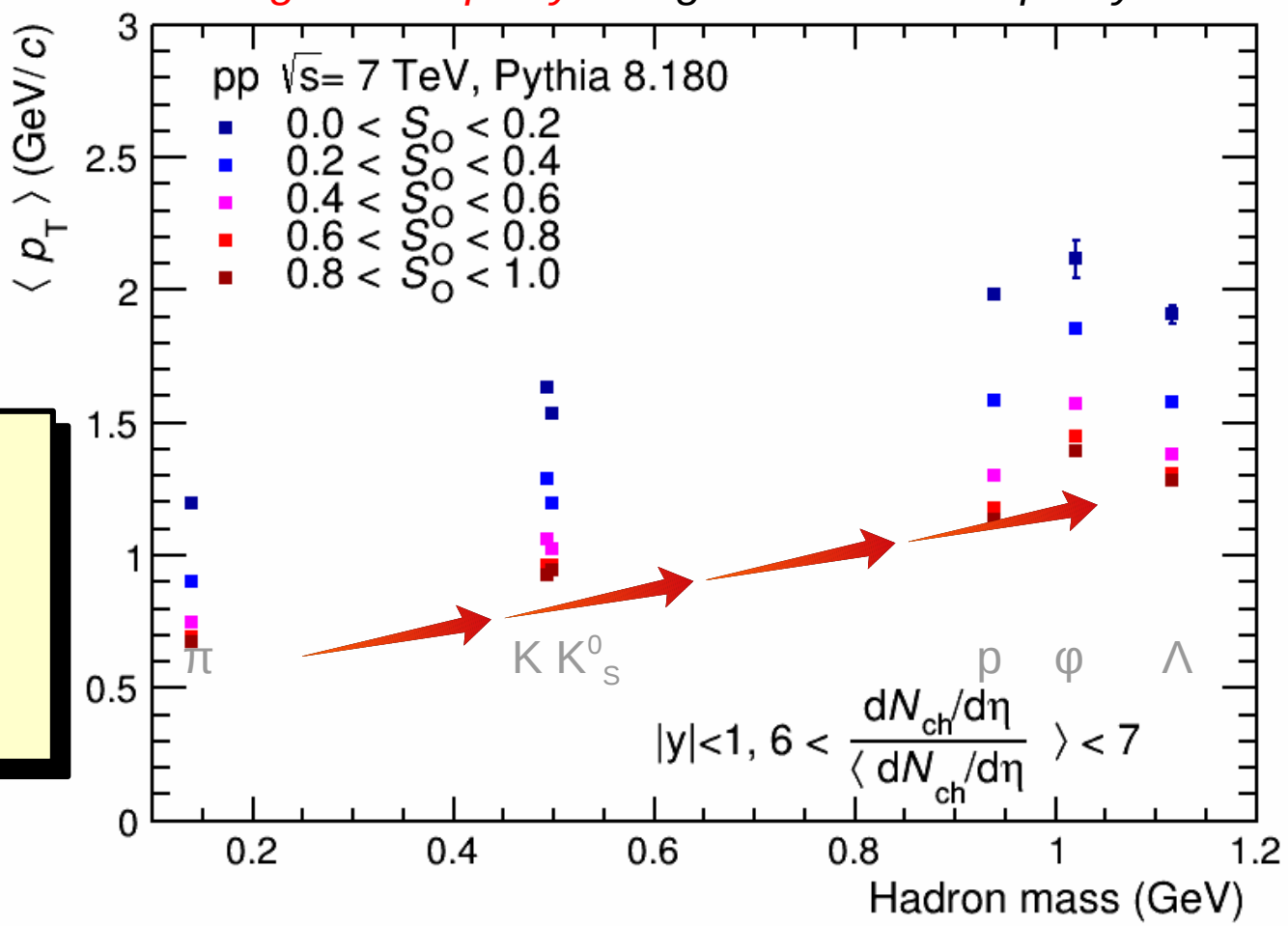

- An increase of the <p_T> with increasing hadron mass is observed for the different event classes.
- The harder the event, the larger the effect (larger <p_T>).

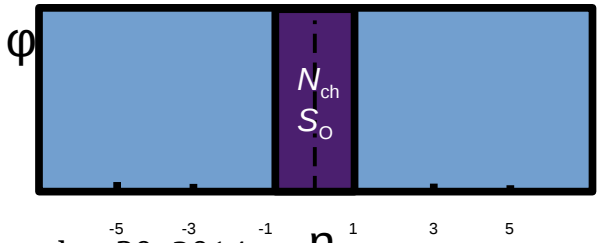

*The inclusive case (w/o any cut on S_O) roughly follows the magenta points

Mass ordering

If baryons and mesons are observed separately, It seems that for isotropic events the $\langle p_T \rangle$ increases linearly with the hadron mass.

High mid-rapidity charged hadron multiplicity

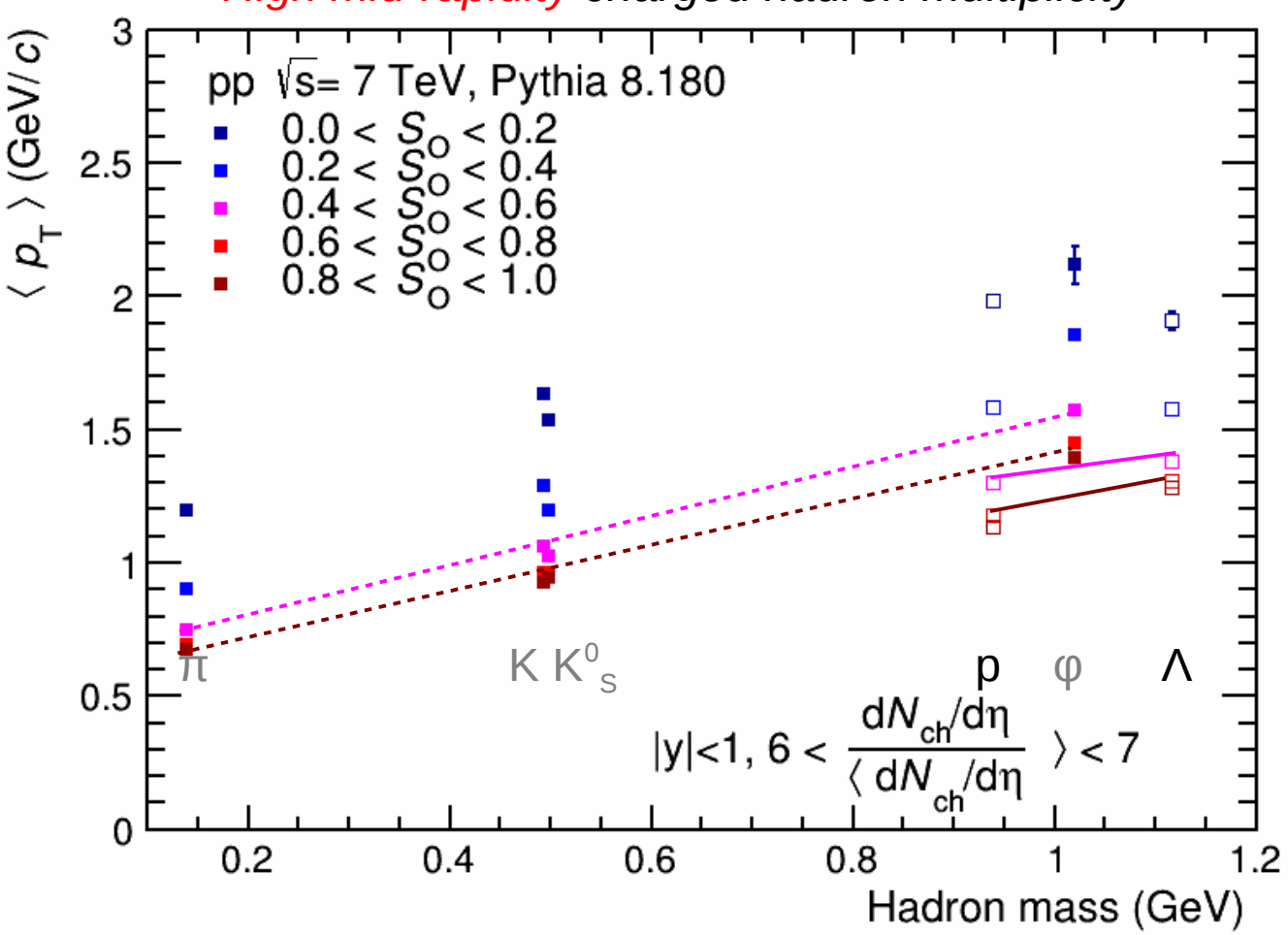

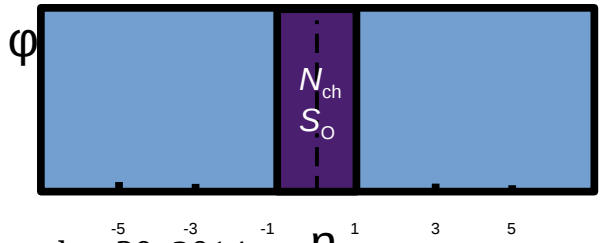

*The inclusive case (w/o any cut on S_O) roughly follows the magenta points

Mass ordering

If baryons and mesons are observed separately, It seems that for isotropic events the $\langle p_T \rangle$ increases linearly with the hadron mass.

The mass ordering seems to be broken for baryons in events enriched with high p_T jets (S_O<0.4).

Are these features exclusive of flow-like caused by a partonic mechanism? It would be very interesting to repeat this analysis in data and in EPOS (hydro).

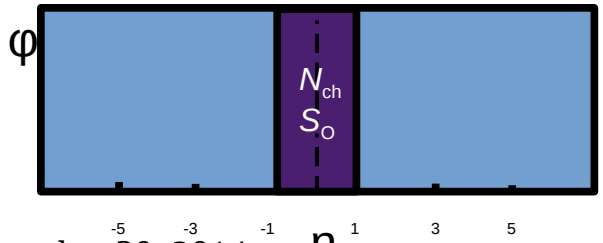

High mid-rapidity charged hadron multiplicity

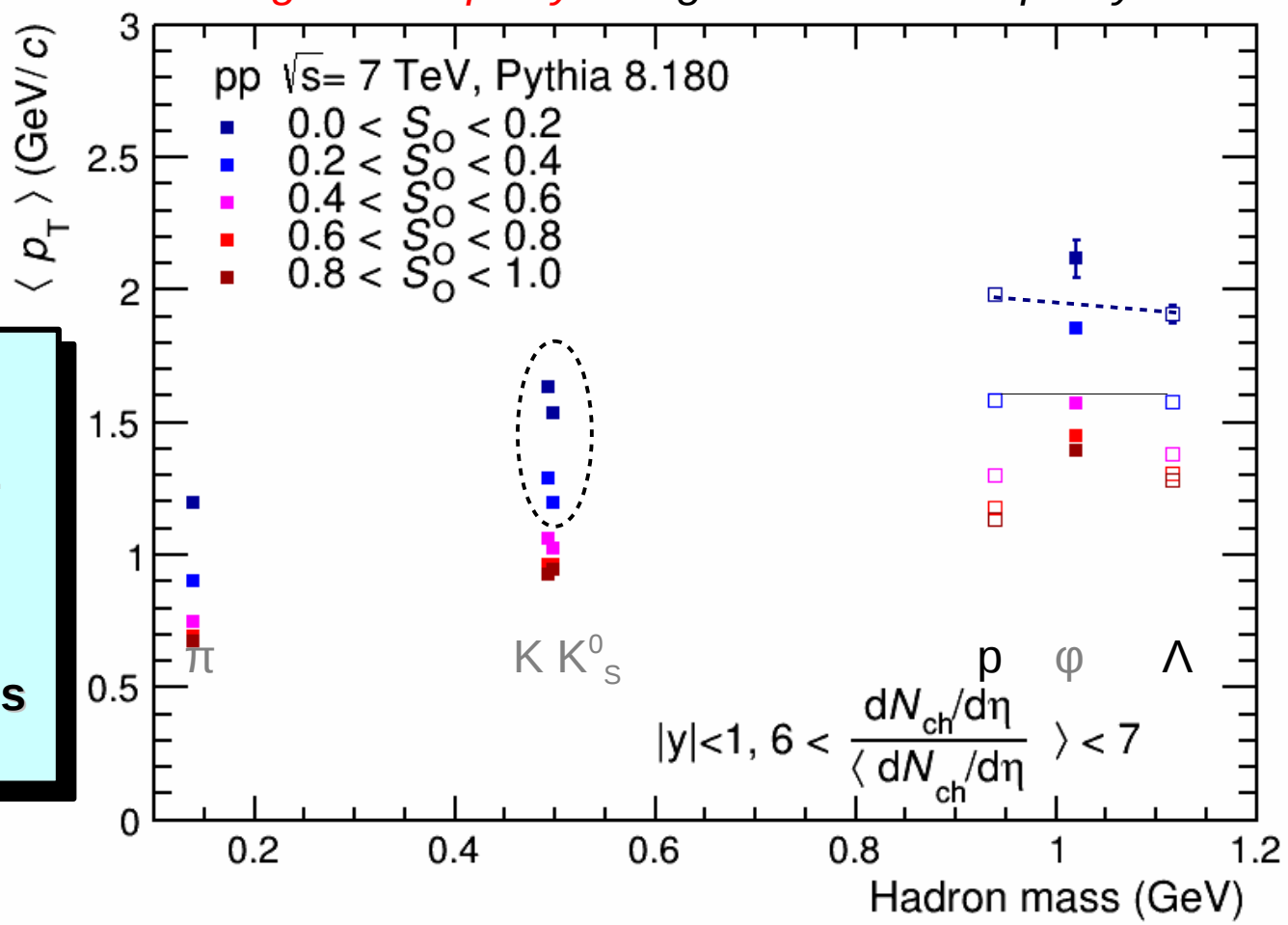

*The inclusive case (w/o any cut on S_O) roughly follows the magenta points

Event shapes are observables which together with multiplicity can be used to perform detailed studies of the pp and p-Pb collisions.

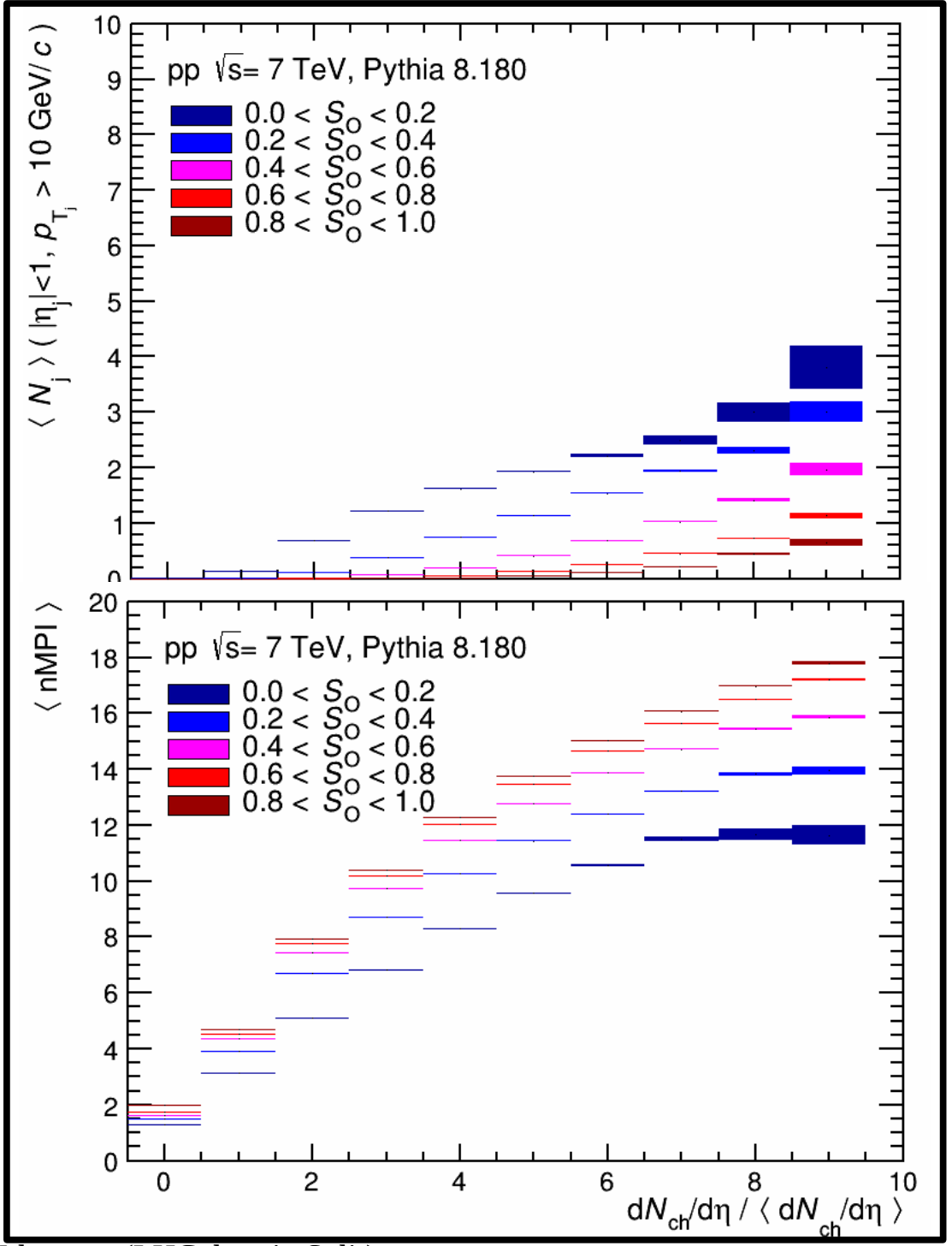

Summary

Event shapes are observables which together with multiplicity can be used to perform detailed studies of the

Among other applications, this separation could be used for a better understanding of the mechanism which originates the flow patterns observed in pp and p-Pb data.

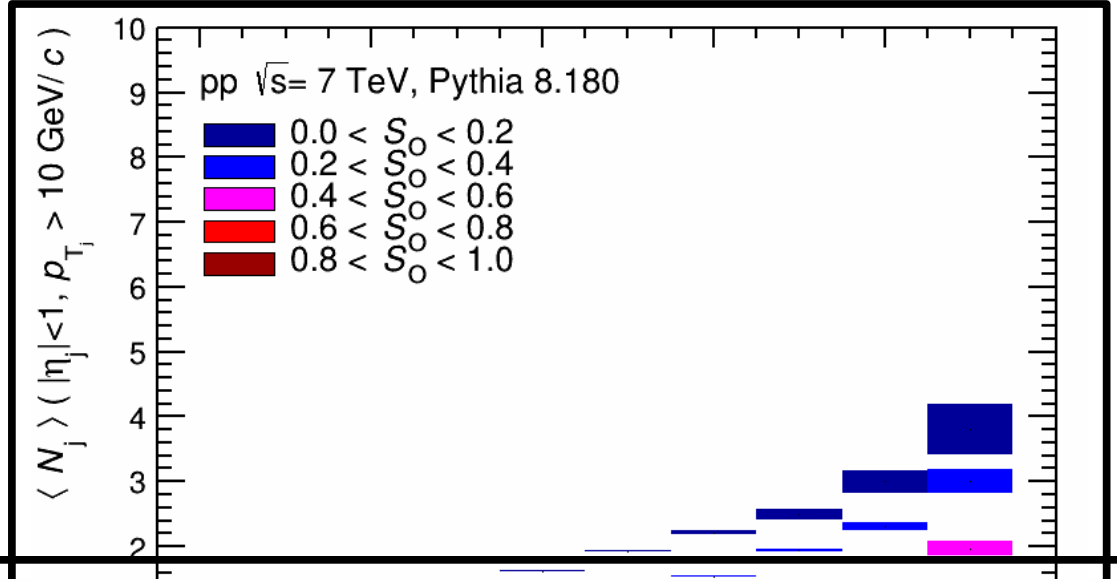

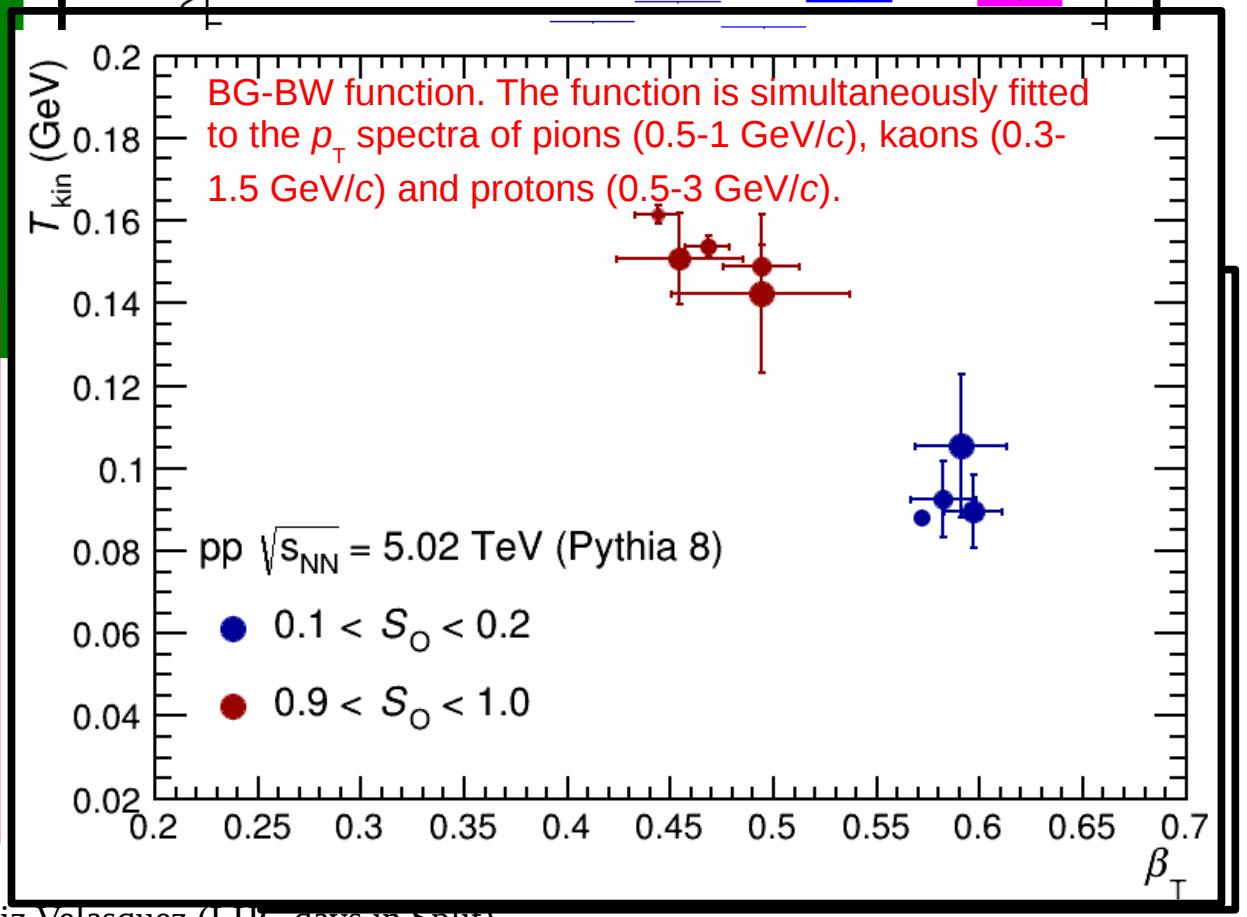

Summary

Event shapes are observables

which

multip

perfor

Among

separation could be used for a better understanding of the mechanism which originates the flow patterns observed in pp and p-Pb data.

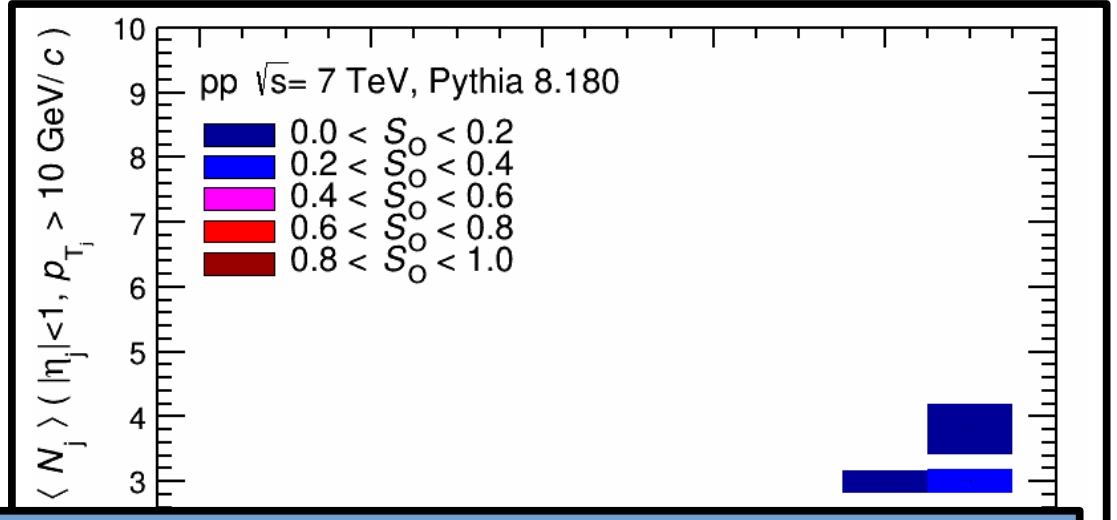

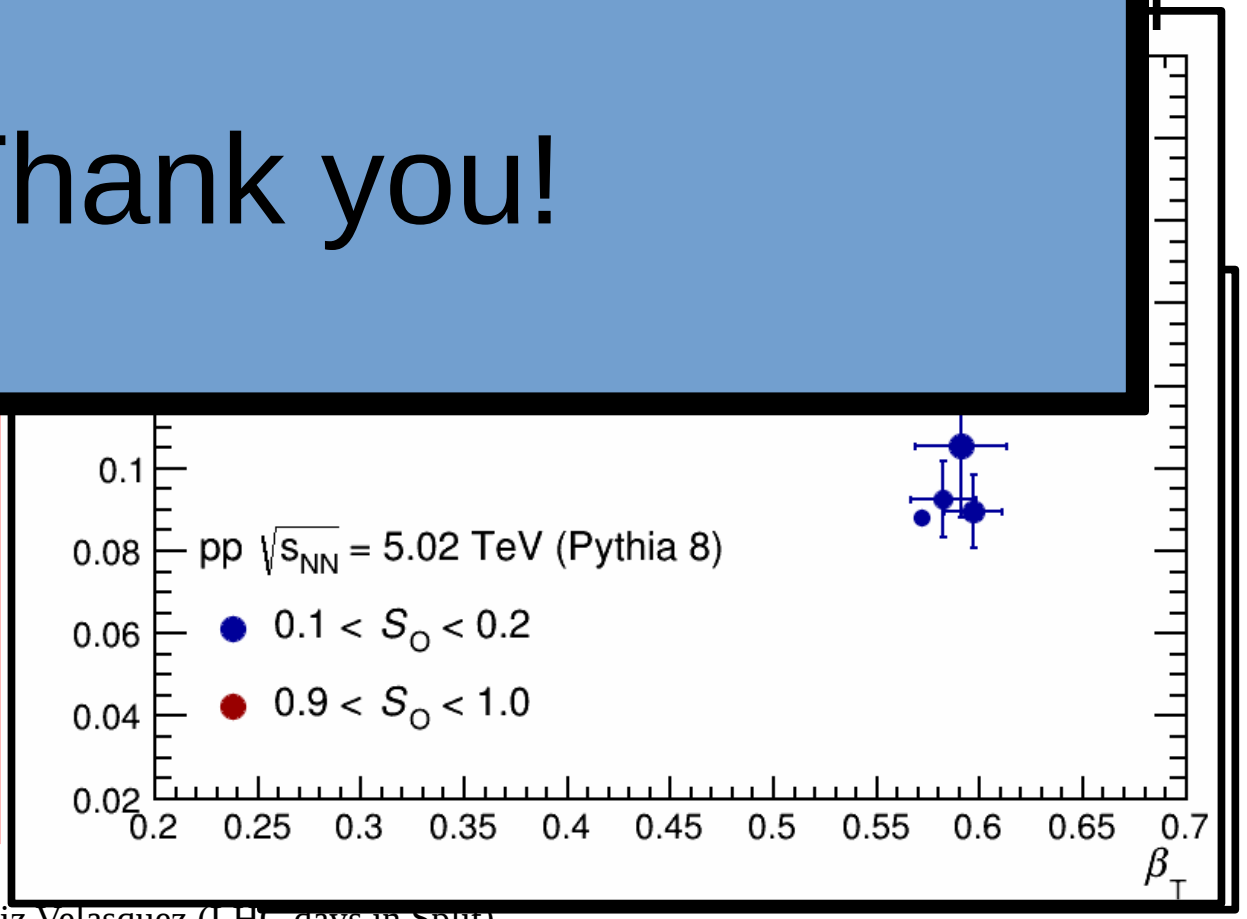

Thank you!

Backup

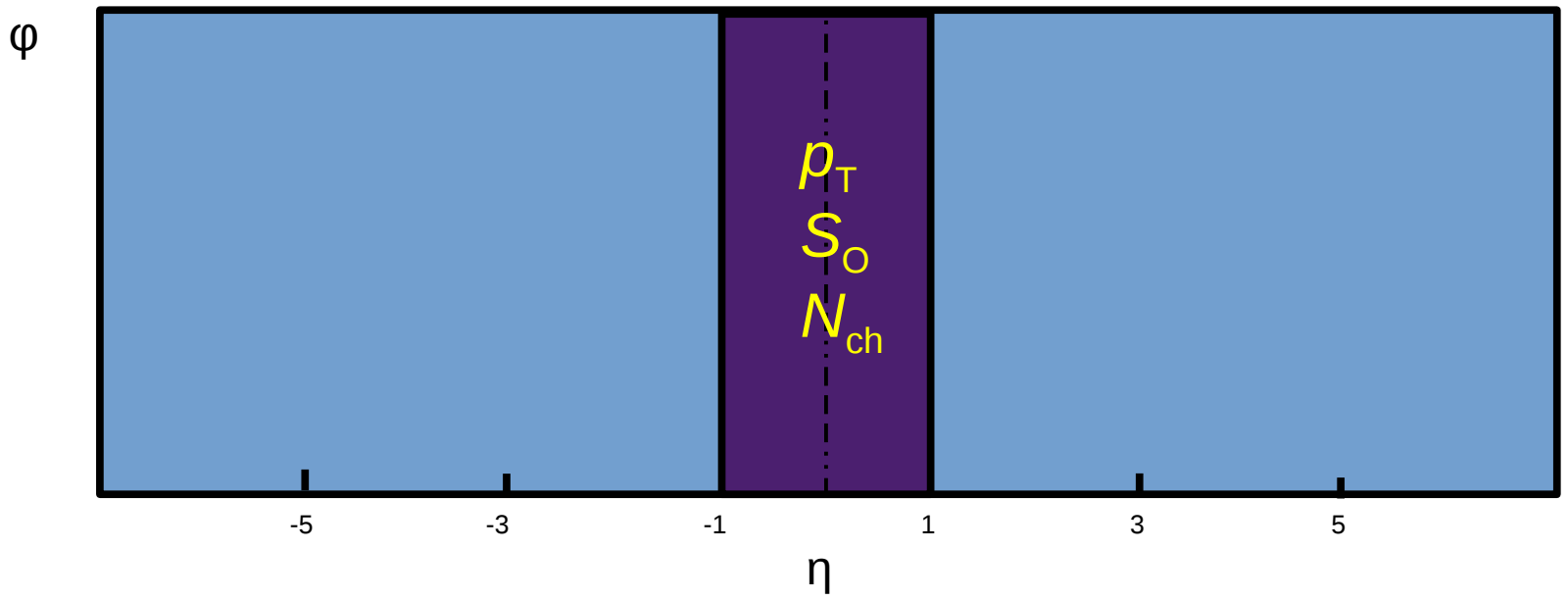

The next slides show the results when all the observables are calculated in the same pseudorapidity interval (|η|<1).

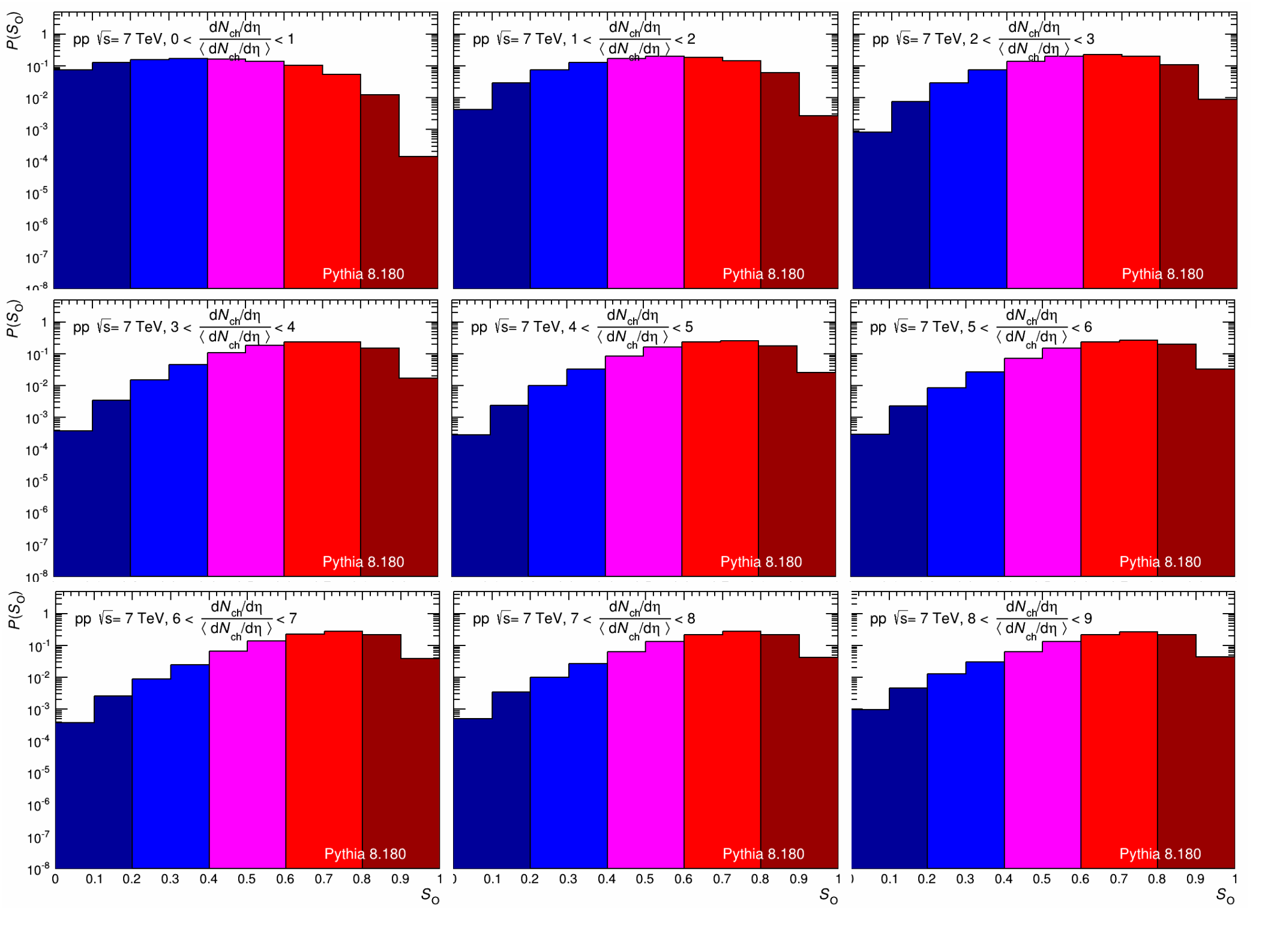
pp √s= 7 TeV, 0 < dN_ch/dη / ⟨ dN_ch/dη ⟩ < 1
pp √s= 7 TeV, 1 < dN_ch/dη / ⟨ dN_ch/dη ⟩ < 2
pp √s= 7 TeV, 2 < dN_ch/dη / ⟨ dN_ch/dη ⟩ < 3
pp √s= 7 TeV, 3 < dN_ch/dη / ⟨ dN_ch/dη ⟩ < 4
pp √s= 7 TeV, 4 < dN_ch/dη / ⟨ dN_ch/dη ⟩ < 5
pp √s= 7 TeV, 5 < dN_ch/dη / ⟨ dN_ch/dη ⟩ < 6
pp √s= 7 TeV, 6 < dN_ch/dη / ⟨ dN_ch/dη ⟩ < 7
pp √s= 7 TeV, 7 < dN_ch/dη / ⟨ dN_ch/dη ⟩ < 8
pp √s= 7 TeV, 8 < dN_ch/dη / ⟨ dN_ch/dη ⟩ < 9
Pythia 8.180
P(S_O)
S_O
0 0.1 0.2 0.3 0.4 0.5 0.6 0.7 0.8 0.9 1
1 10^-1 10^-2 10^-3 10^-4 10^-5 10^-6 10^-7 10^-8

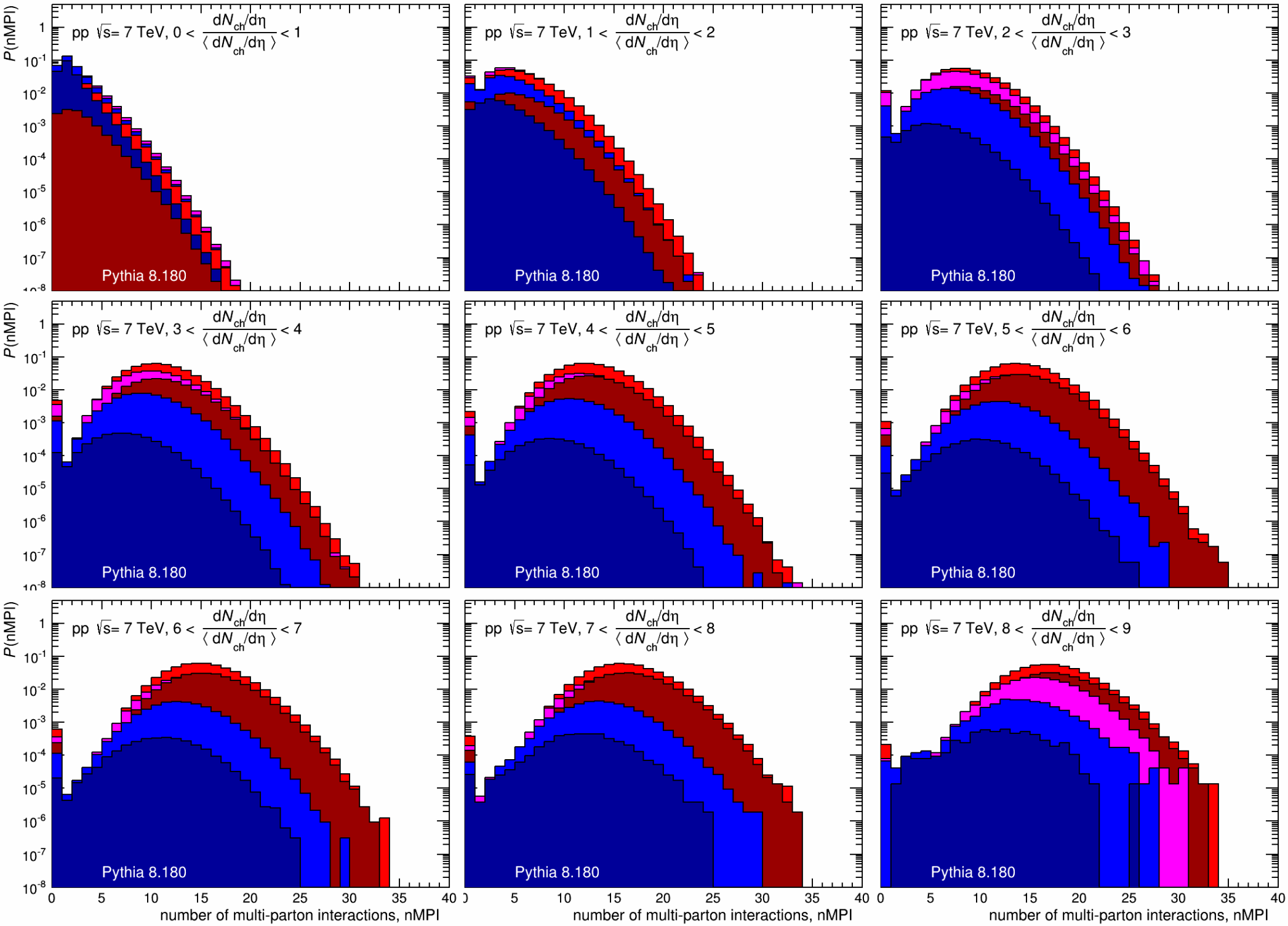
pp √s= 7 TeV, 0 < dN_ch/dη / ⟨ dN_ch/dη ⟩ < 1
pp √s= 7 TeV, 1 < dN_ch/dη / ⟨ dN_ch/dη ⟩ < 2
pp √s= 7 TeV, 2 < dN_ch/dη / ⟨ dN_ch/dη ⟩ < 3
pp √s= 7 TeV, 3 < dN_ch/dη / ⟨ dN_ch/dη ⟩ < 4
pp √s= 7 TeV, 4 < dN_ch/dη / ⟨ dN_ch/dη ⟩ < 5
pp √s= 7 TeV, 5 < dN_ch/dη / ⟨ dN_ch/dη ⟩ < 6
pp √s= 7 TeV, 6 < dN_ch/dη / ⟨ dN_ch/dη ⟩ < 7
pp √s= 7 TeV, 7 < dN_ch/dη / ⟨ dN_ch/dη ⟩ < 8
pp √s= 7 TeV, 8 < dN_ch/dη / ⟨ dN_ch/dη ⟩ < 9
Pythia 8.180
P(nMPI)
number of multi-parton interactions, nMPI
0
5
10
15
20
25
30
35
40
1
10^-1
10^-2
10^-3
10^-4
10^-5
10^-6
10^-7
10^-8

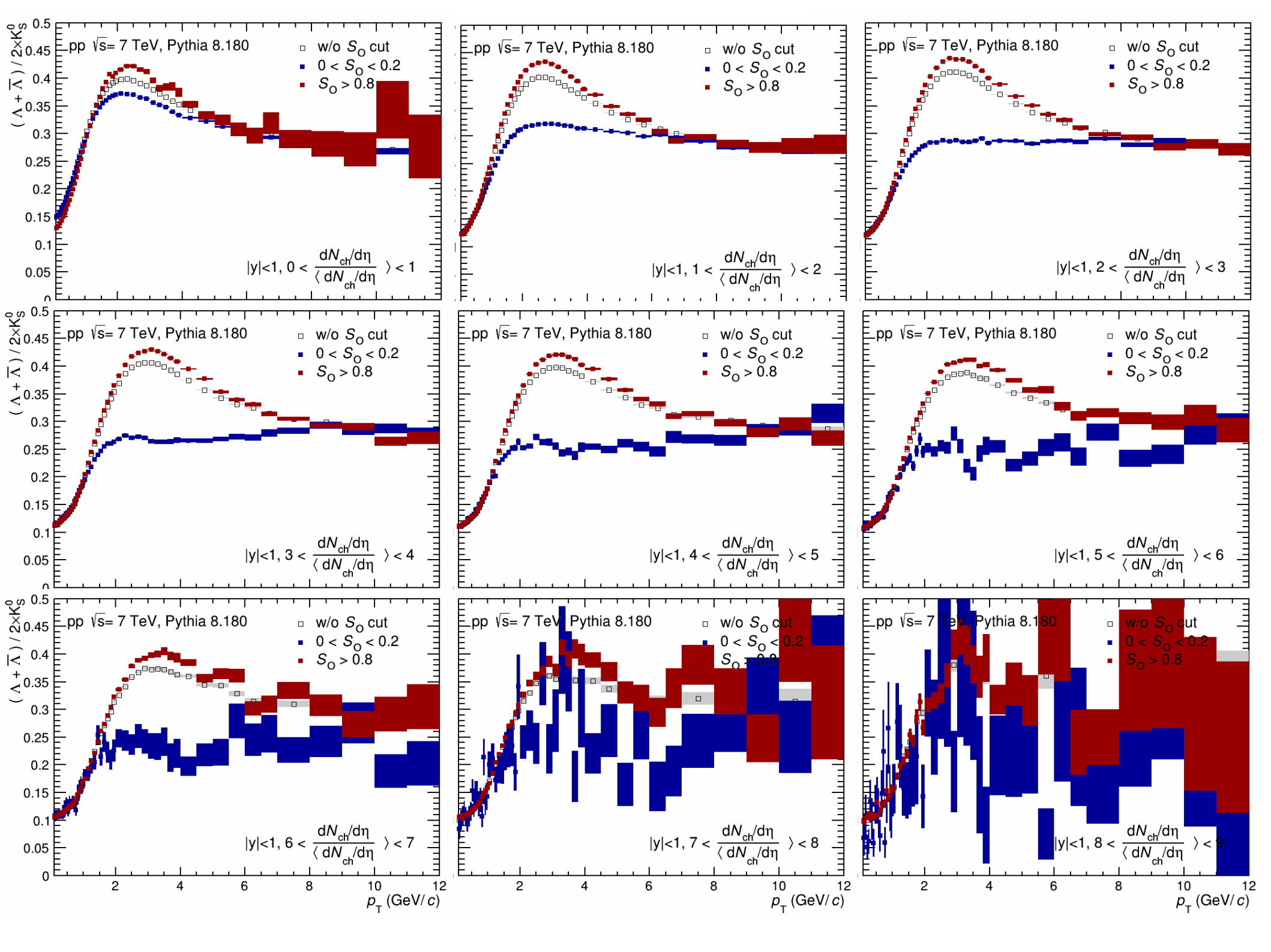
pp √s= 7 TeV, Pythia 8.180
w/o S_O cut
$0 < S_O < 0.2$
$S_O > 0.8$
$(\Lambda + \bar{\Lambda}) / 2\times K^0_S$
p_T (GeV/c)
|y|<1, 0 < $\frac{dN_{ch}/d\eta}{\langle dN_{ch}/d\eta \rangle}$ < 1
|y|<1, 1 < $\frac{dN_{ch}/d\eta}{\langle dN_{ch}/d\eta \rangle}$ < 2
|y|<1, 2 < $\frac{dN_{ch}/d\eta}{\langle dN_{ch}/d\eta \rangle}$ < 3
|y|<1, 3 < $\frac{dN_{ch}/d\eta}{\langle dN_{ch}/d\eta \rangle}$ < 4
|y|<1, 4 < $\frac{dN_{ch}/d\eta}{\langle dN_{ch}/d\eta \rangle}$ < 5
|y|<1, 5 < $\frac{dN_{ch}/d\eta}{\langle dN_{ch}/d\eta \rangle}$ < 6
|y|<1, 6 < $\frac{dN_{ch}/d\eta}{\langle dN_{ch}/d\eta \rangle}$ < 7
|y|<1, 7 < $\frac{dN_{ch}/d\eta}{\langle dN_{ch}/d\eta \rangle}$ < 8
|y|<1, 8 < $\frac{dN_{ch}/d\eta}{\langle dN_{ch}/d\eta \rangle}$ < 9

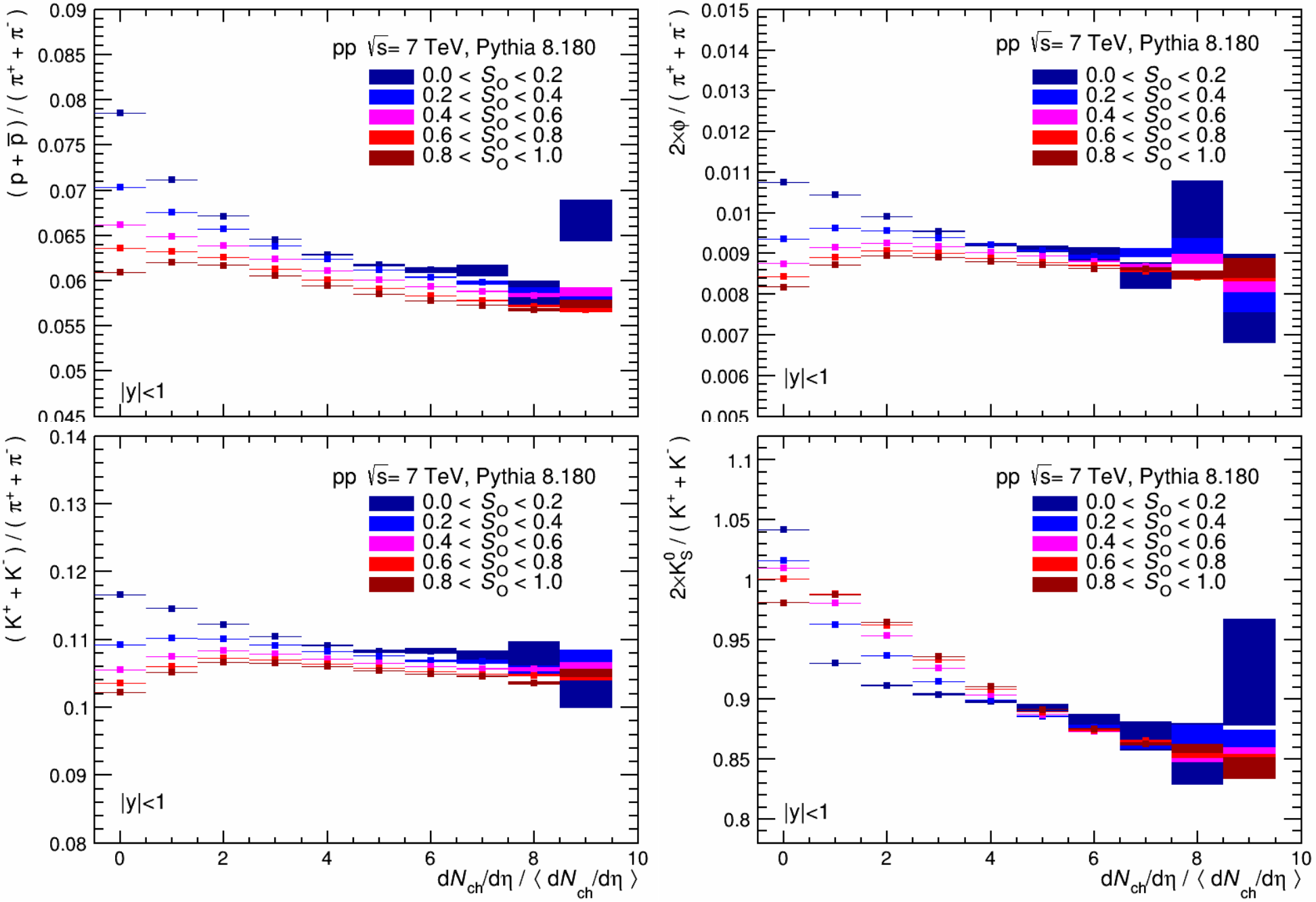

*The inclusive case (w/o any cut on S_O) roughly follows the magenta points

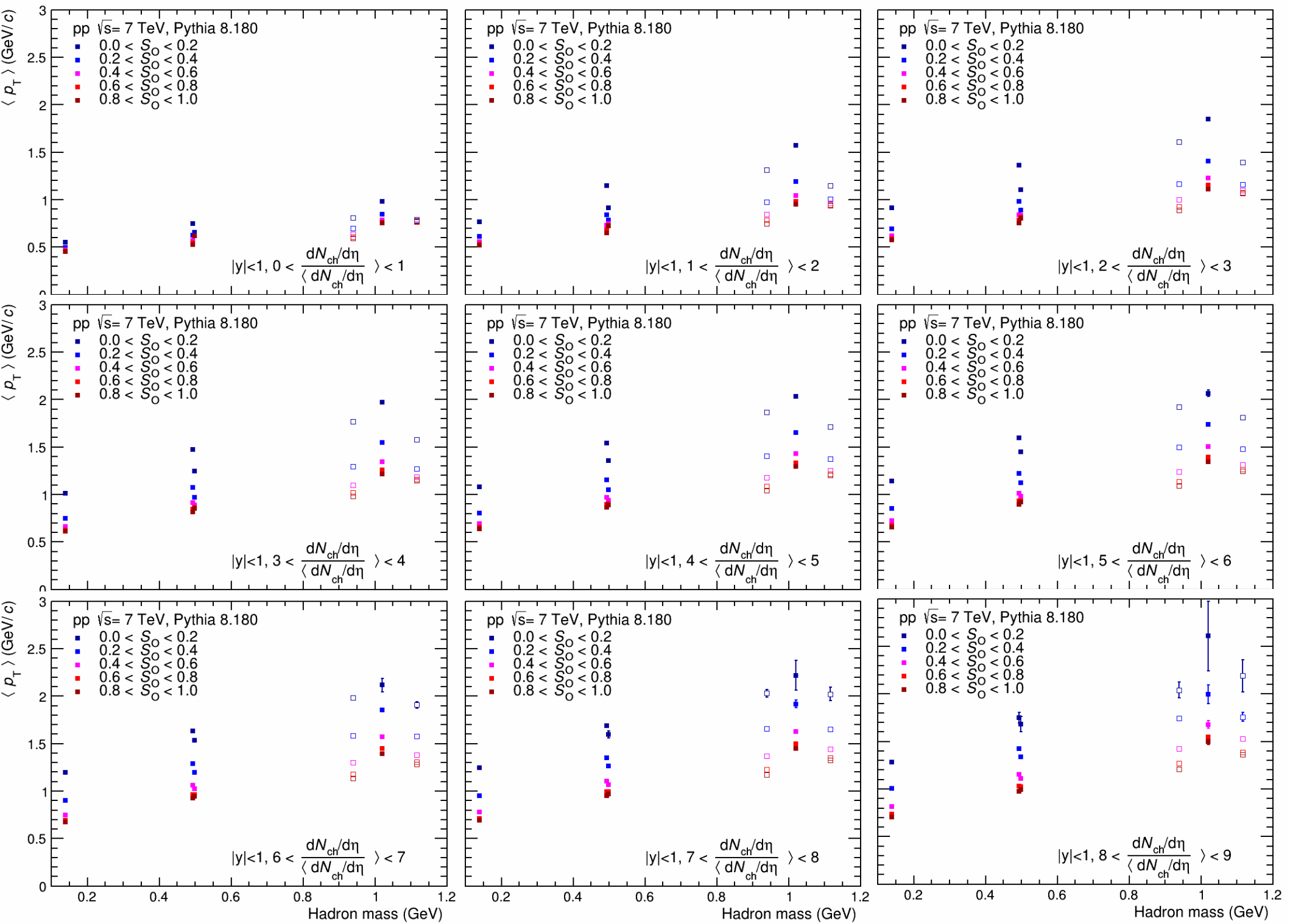

*The inclusive case (w/o any cut on S_O) roughly follows the magenta points

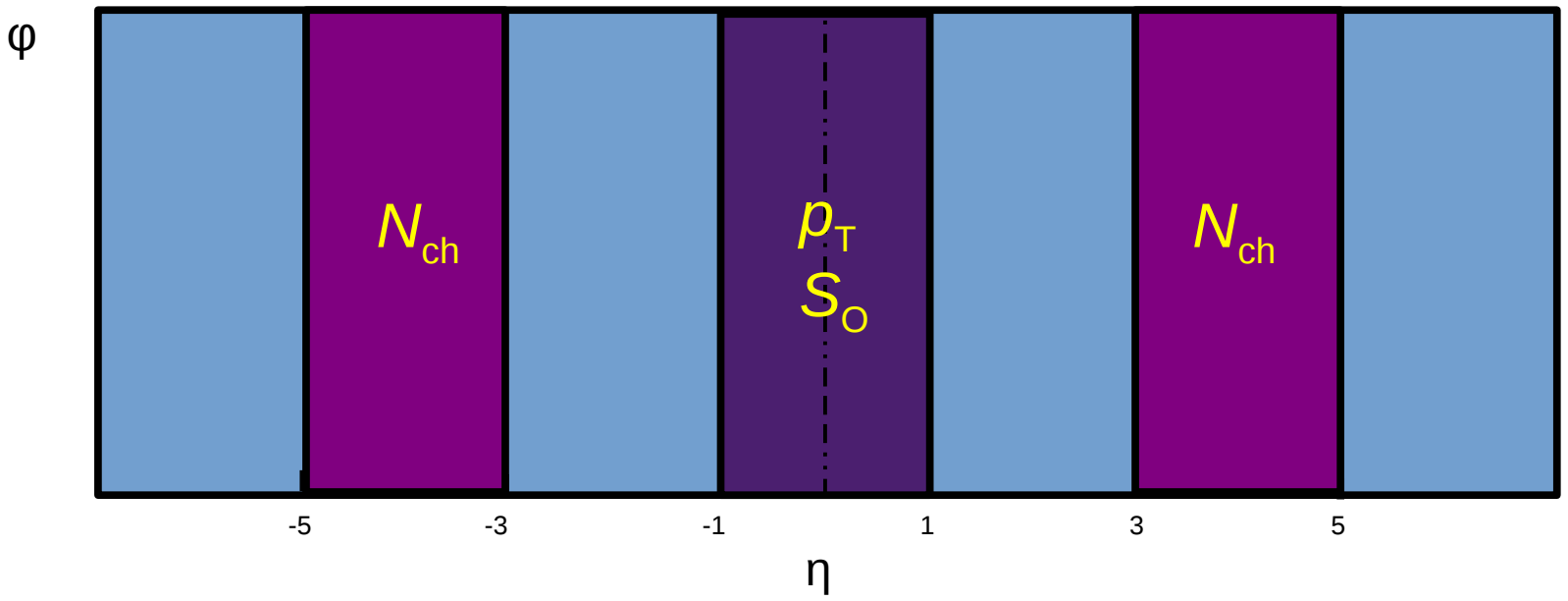

The next slides show the results when the transverse momentum spectrum and spherocity are calculated at mid-pseudorapidity (|η|<1) and multiplicity is computed at forward pseudorapidity (3<|η|<5).

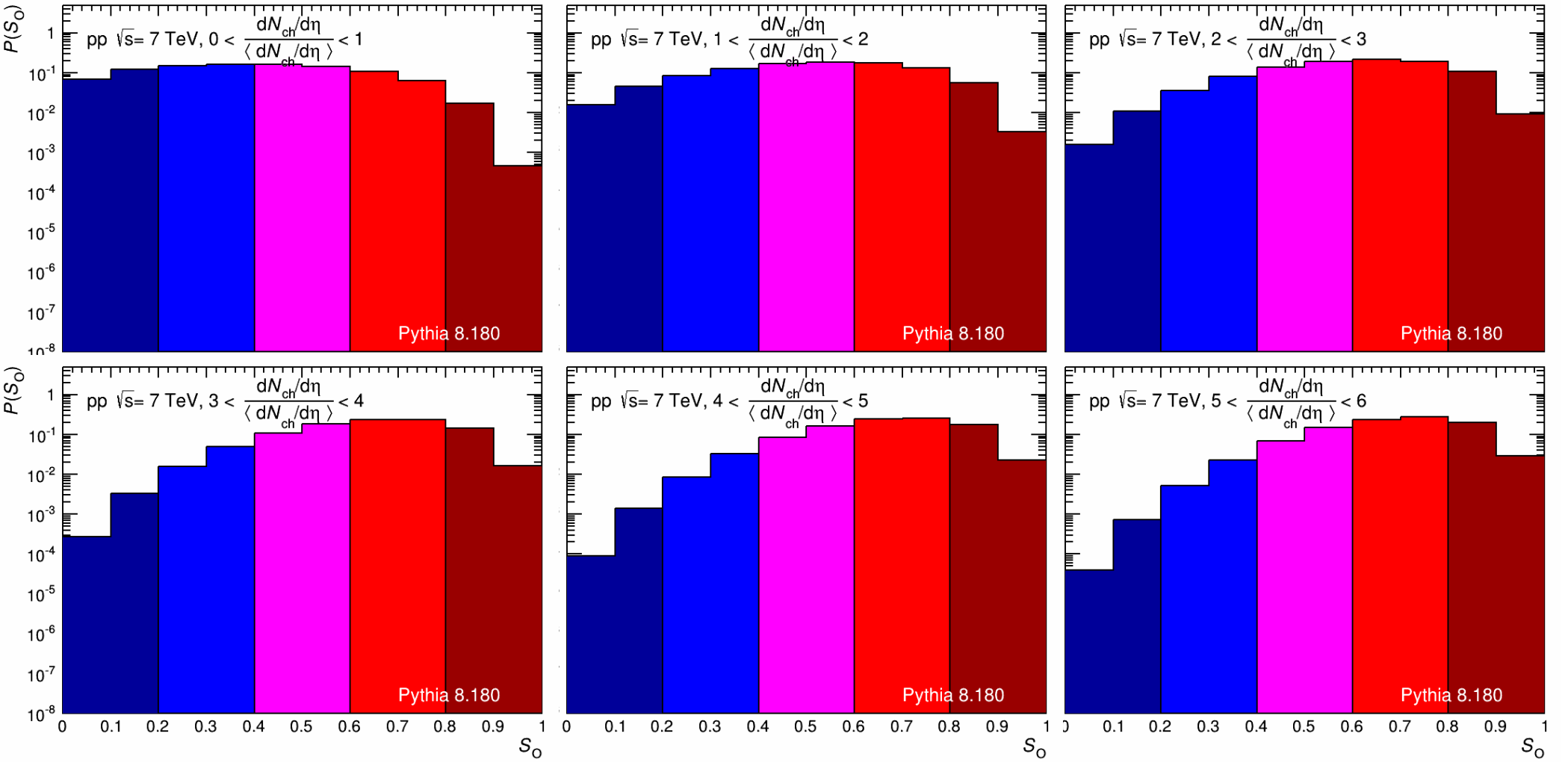
pp √s= 7 TeV, 0 < dN_ch/dη / ⟨ dN_ch/dη ⟩ < 1
pp √s= 7 TeV, 1 < dN_ch/dη / ⟨ dN_ch/dη ⟩ < 2
pp √s= 7 TeV, 2 < dN_ch/dη / ⟨ dN_ch/dη ⟩ < 3
pp √s= 7 TeV, 3 < dN_ch/dη / ⟨ dN_ch/dη ⟩ < 4
pp √s= 7 TeV, 4 < dN_ch/dη / ⟨ dN_ch/dη ⟩ < 5
pp √s= 7 TeV, 5 < dN_ch/dη / ⟨ dN_ch/dη ⟩ < 6
Pythia 8.180
P(S_O)
S_O

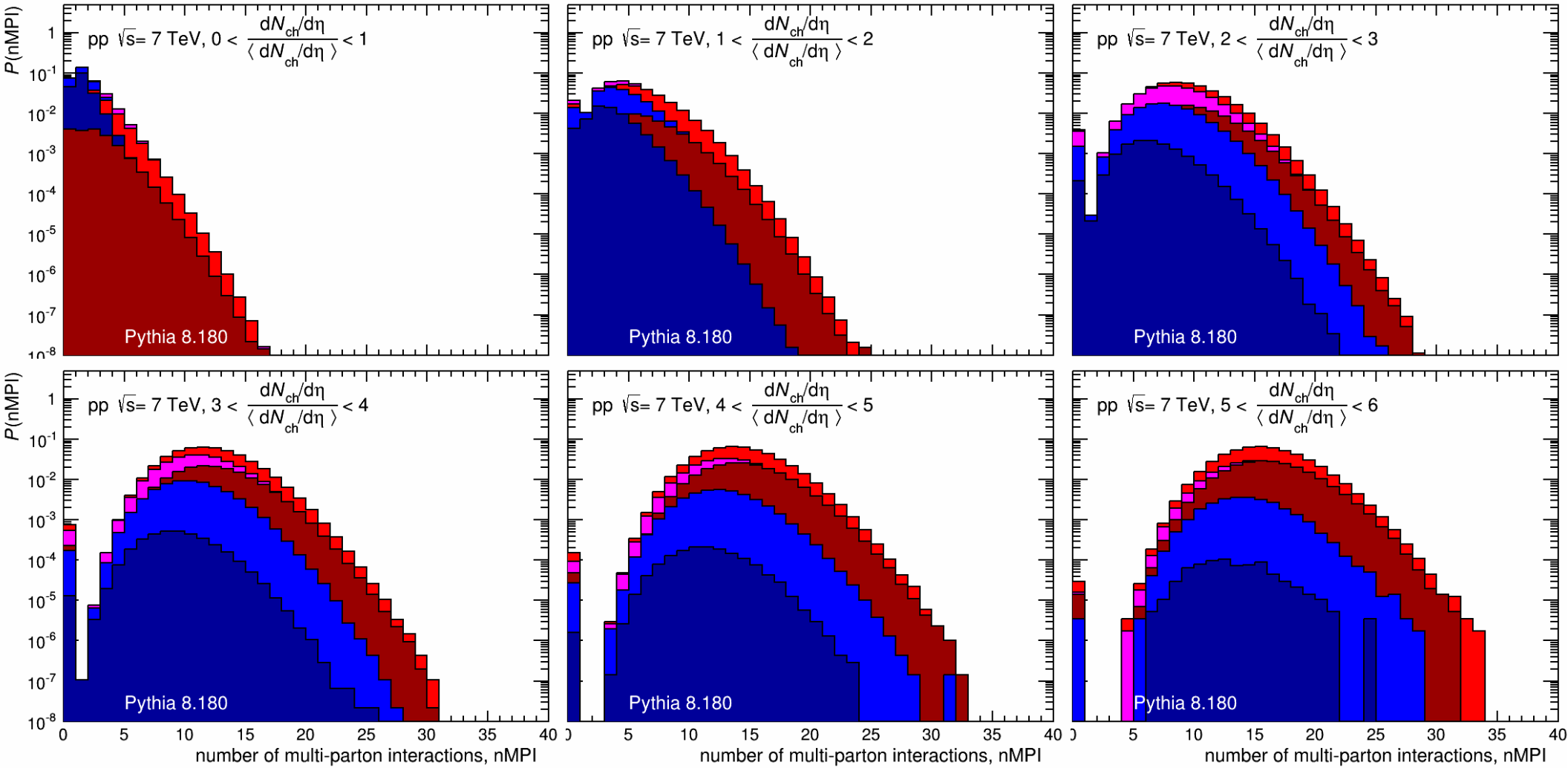
P(nMPI)
pp √s= 7 TeV, 0 < dN_ch/dη / ⟨ dN_ch/dη ⟩ < 1
pp √s= 7 TeV, 1 < dN_ch/dη / ⟨ dN_ch/dη ⟩ < 2
pp √s= 7 TeV, 2 < dN_ch/dη / ⟨ dN_ch/dη ⟩ < 3
pp √s= 7 TeV, 3 < dN_ch/dη / ⟨ dN_ch/dη ⟩ < 4
pp √s= 7 TeV, 4 < dN_ch/dη / ⟨ dN_ch/dη ⟩ < 5
pp √s= 7 TeV, 5 < dN_ch/dη / ⟨ dN_ch/dη ⟩ < 6
Pythia 8.180
number of multi-parton interactions, nMPI

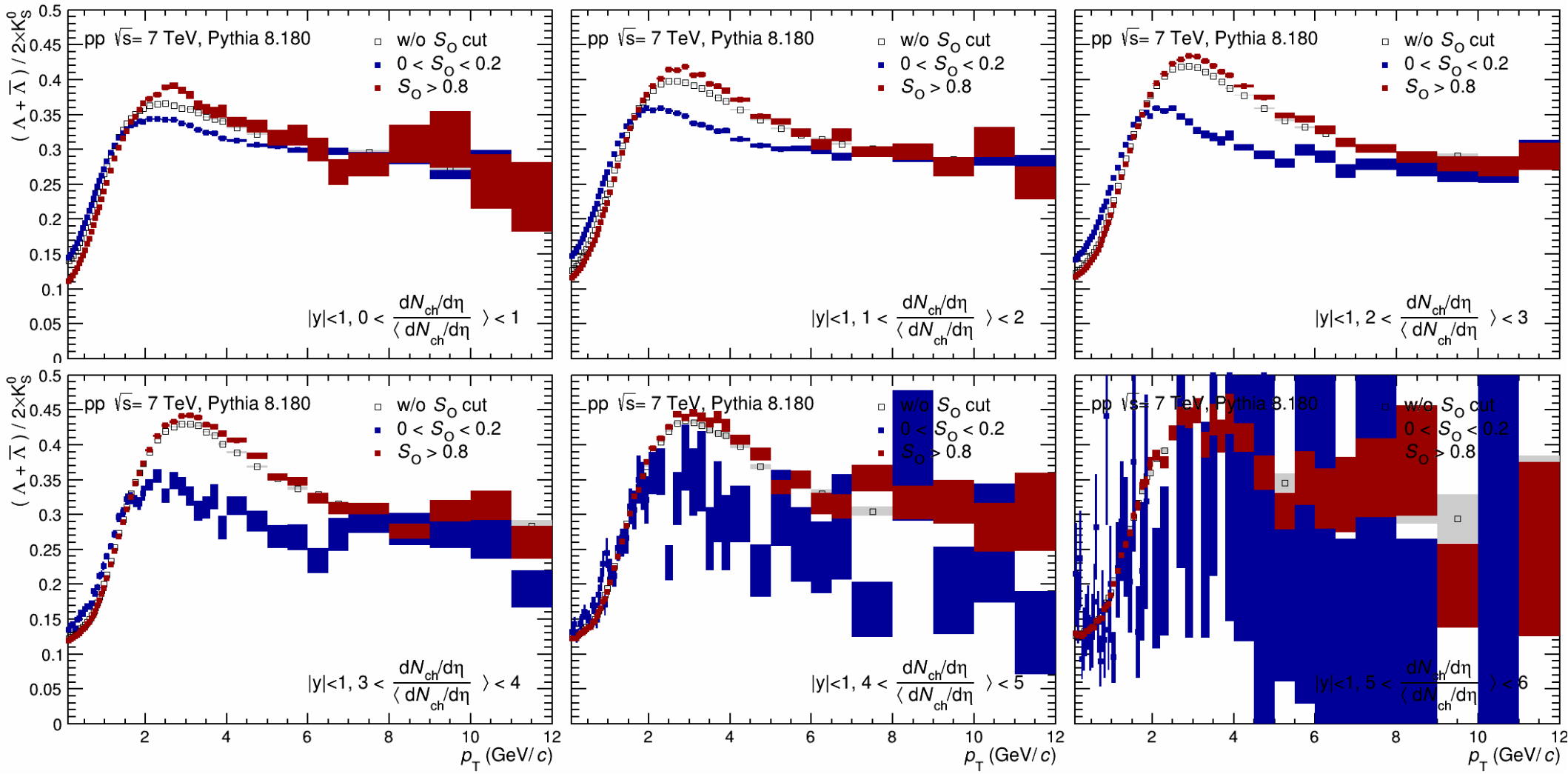
pp √s= 7 TeV, Pythia 8.180
w/o S_O cut
0 < S_O < 0.2
S_O > 0.8
$(\Lambda+\bar{\Lambda})/2\times K^0_S$
|y|<1, 0 < $\frac{dN_{ch}/d\eta}{\langle dN_{ch}/d\eta \rangle}$ < 1
|y|<1, 1 < $\frac{dN_{ch}/d\eta}{\langle dN_{ch}/d\eta \rangle}$ < 2
|y|<1, 2 < $\frac{dN_{ch}/d\eta}{\langle dN_{ch}/d\eta \rangle}$ < 3
|y|<1, 3 < $\frac{dN_{ch}/d\eta}{\langle dN_{ch}/d\eta \rangle}$ < 4
|y|<1, 4 < $\frac{dN_{ch}/d\eta}{\langle dN_{ch}/d\eta \rangle}$ < 5
|y|<1, 5 < $\frac{dN_{ch}/d\eta}{\langle dN_{ch}/d\eta \rangle}$ < 6
p_T (GeV/c)

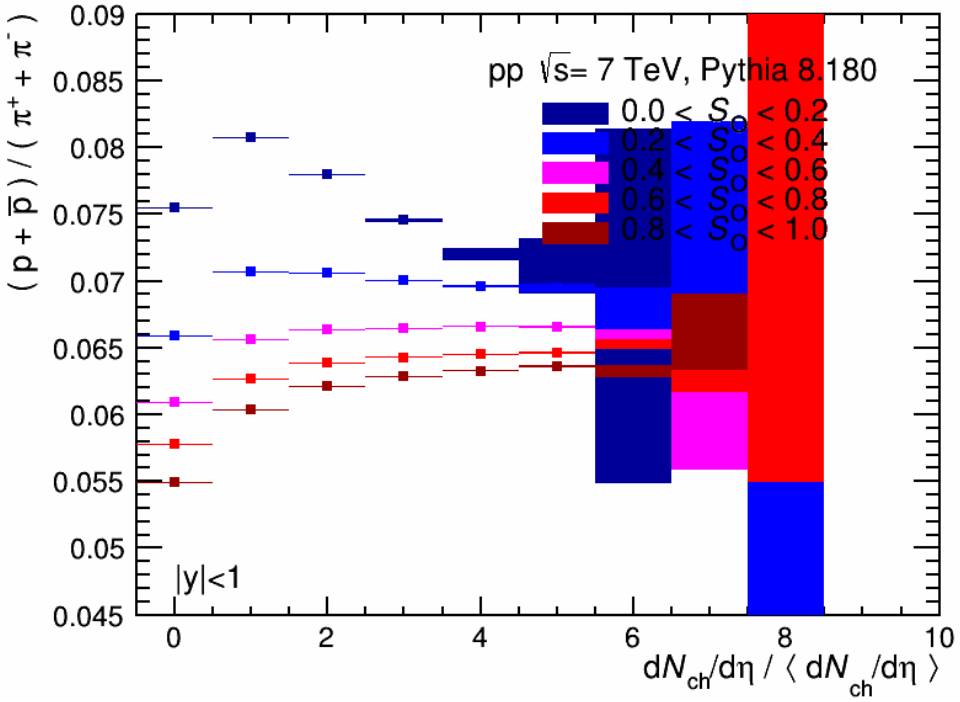
pp √s= 7 TeV, Pythia 8.180
0.0 < S_o < 0.2
0.2 < S_o < 0.4
0.4 < S_o < 0.6
0.6 < S_o < 0.8
0.8 < S_o < 1.0
|y|<1
(p + p̄) / (π⁺ + π⁻)
dN_ch/dη / ⟨ dN_ch/dη ⟩

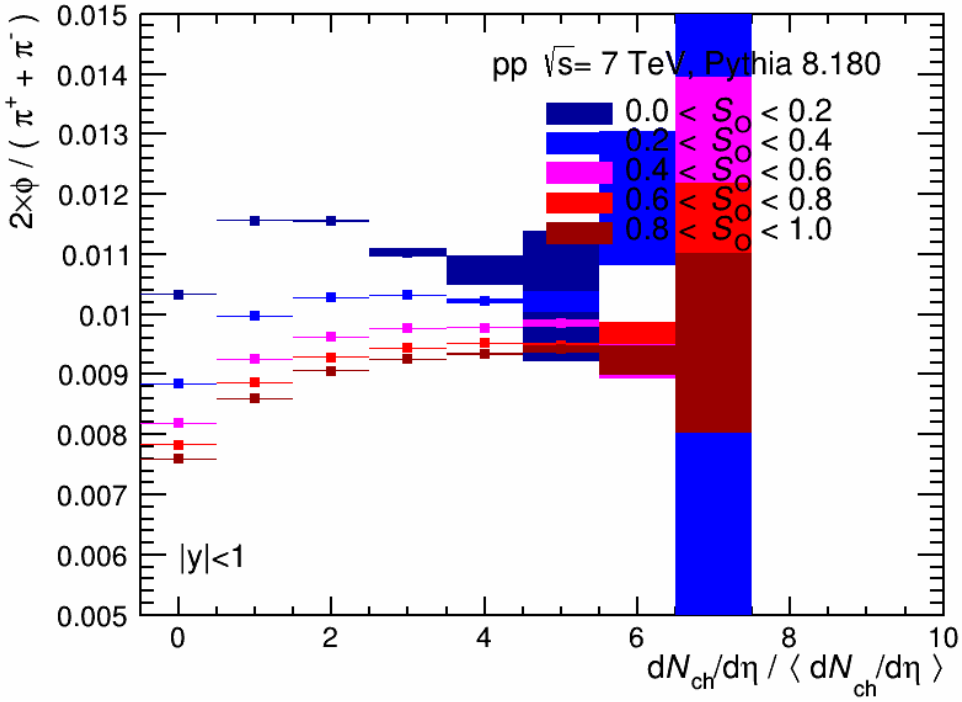
pp √s= 7 TeV, Pythia 8.180
0.0 < S_o < 0.2
0.2 < S_o < 0.4
0.4 < S_o < 0.6
0.6 < S_o < 0.8
0.8 < S_o < 1.0
|y|<1
2×φ / (π⁺ + π⁻)
dN_ch/dη / ⟨ dN_ch/dη ⟩

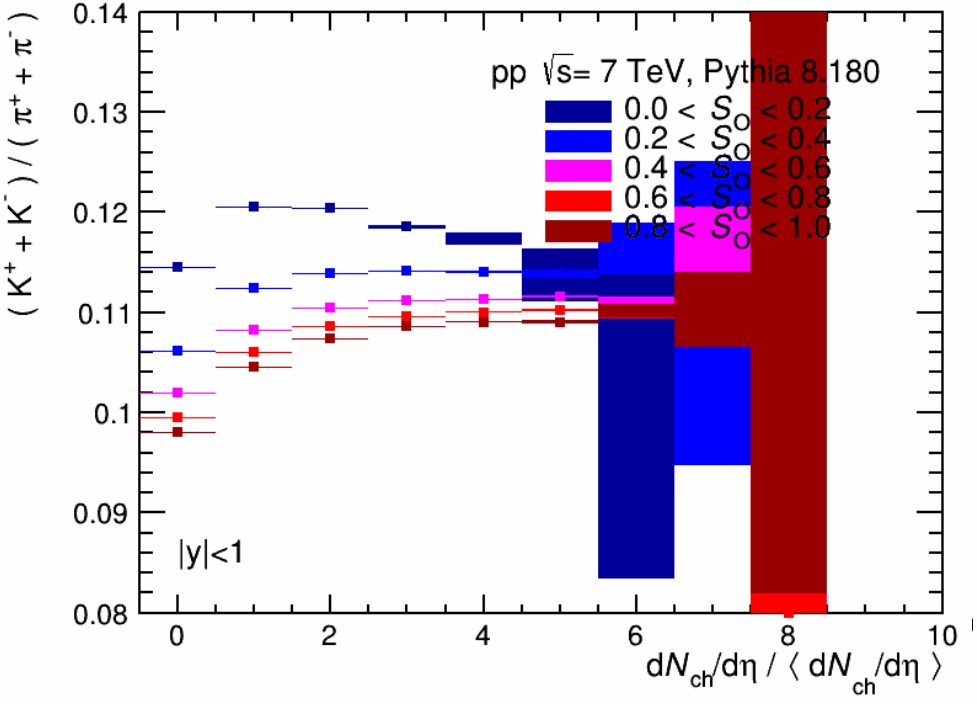
pp √s= 7 TeV, Pythia 8.180
0.0 < S_o < 0.2
0.2 < S_o < 0.4
0.4 < S_o < 0.6
0.6 < S_o < 0.8
0.8 < S_o < 1.0
|y|<1
(K⁺ + K⁻) / (π⁺ + π⁻)
dN_ch/dη / ⟨ dN_ch/dη ⟩

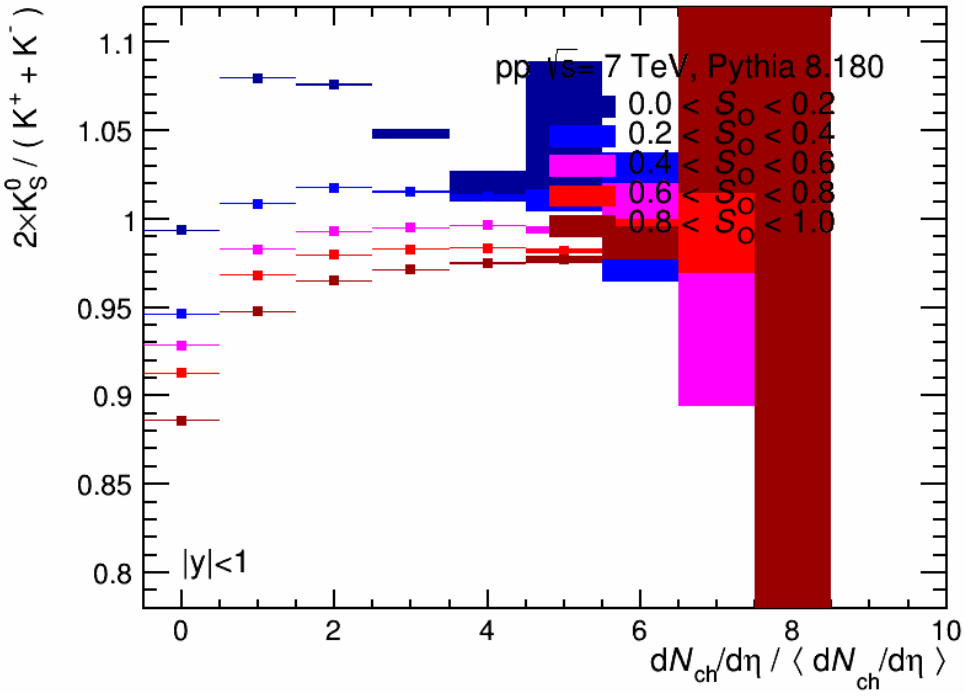
pp √s= 7 TeV, Pythia 8.180
0.0 < S_o < 0.2
0.2 < S_o < 0.4
0.4 < S_o < 0.6
0.6 < S_o < 0.8
0.8 < S_o < 1.0
|y|<1
2×K⁰_S / (K⁺ + K⁻)
dN_ch/dη / ⟨ dN_ch/dη ⟩

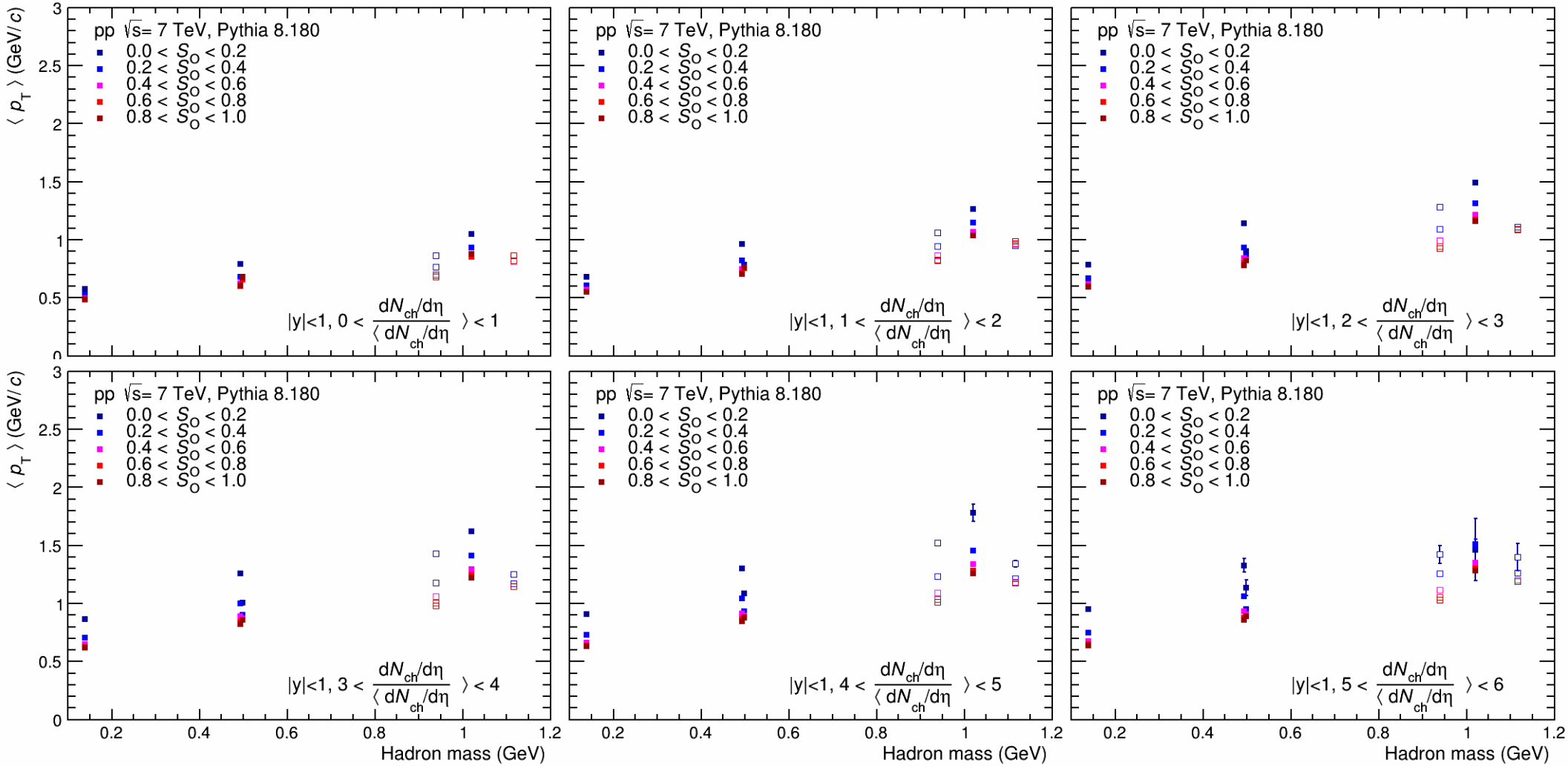
pp √s= 7 TeV, Pythia 8.180
0.0 < S_O < 0.2
0.2 < S_O < 0.4
0.4 < S_O < 0.6
0.6 < S_O < 0.8
0.8 < S_O < 1.0
⟨ p_T ⟩ (GeV/c)
|y|<1, 0 < dN_ch/dη / ⟨ dN_ch/dη ⟩ < 1
|y|<1, 1 < dN_ch/dη / ⟨ dN_ch/dη ⟩ < 2
|y|<1, 2 < dN_ch/dη / ⟨ dN_ch/dη ⟩ < 3
|y|<1, 3 < dN_ch/dη / ⟨ dN_ch/dη ⟩ < 4
|y|<1, 4 < dN_ch/dη / ⟨ dN_ch/dη ⟩ < 5
|y|<1, 5 < dN_ch/dη / ⟨ dN_ch/dη ⟩ < 6
Hadron mass (GeV)

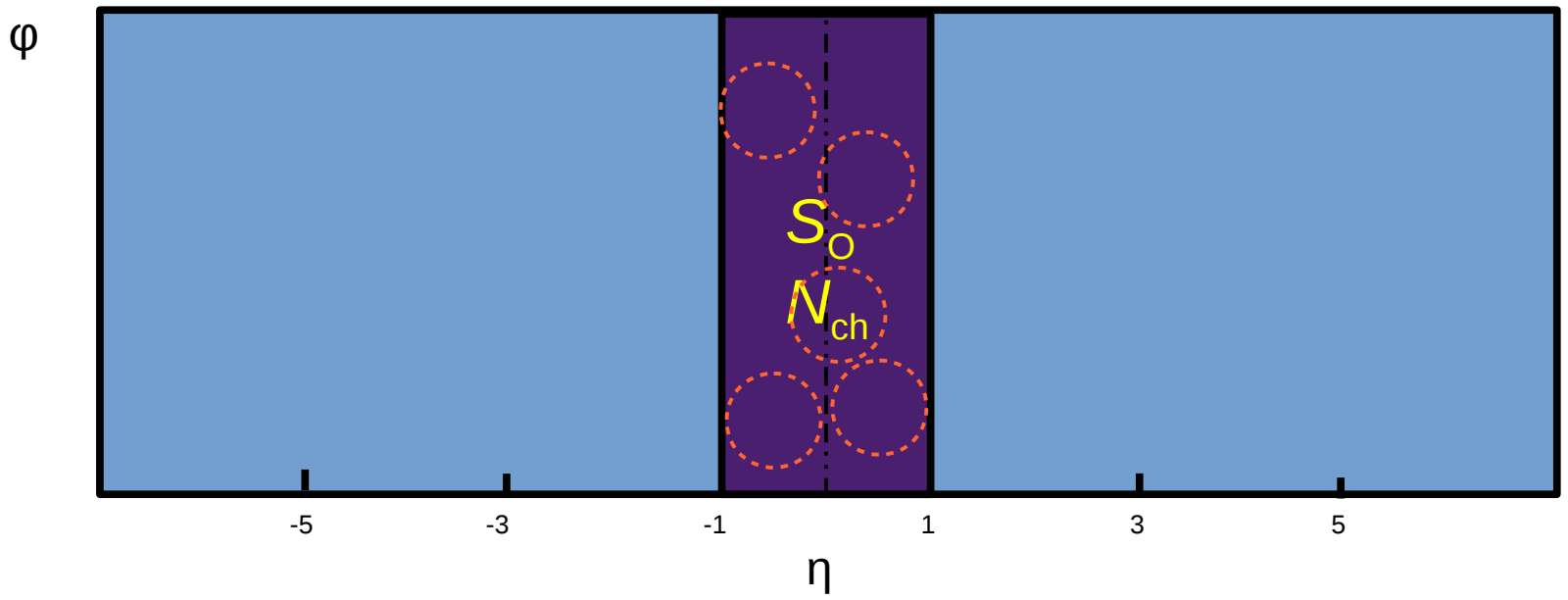

The next slides show the results where multiplicity and spherocity are calculated at mid-pseudorapidity interval (|η|<1). The jet finder is implemented in the same pseudorapidity range.

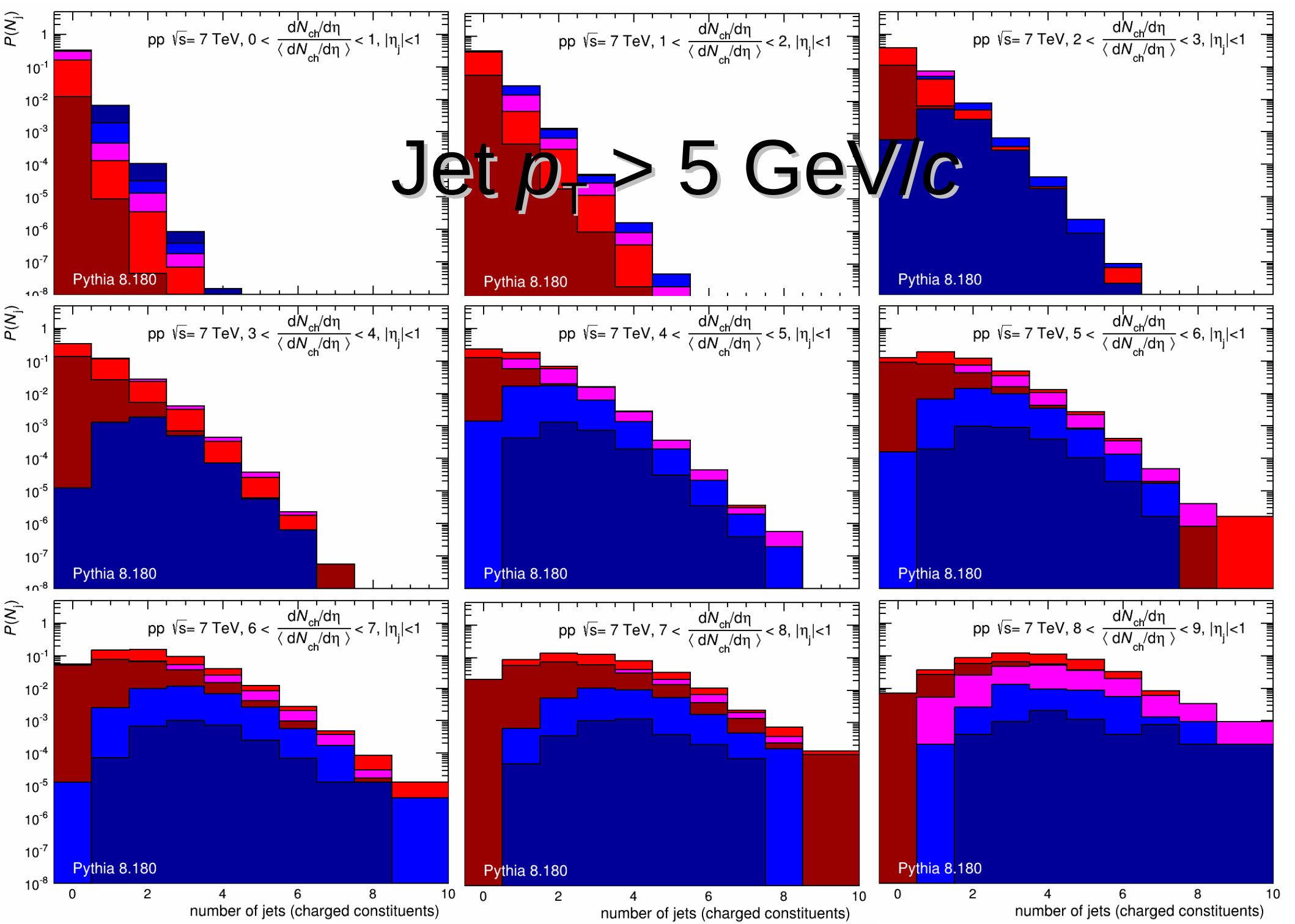
Jet p_T > 5 GeV/c
P(N_j)
pp √s= 7 TeV, 0 < dN_ch/dη / ⟨ dN_ch/dη ⟩ < 1, |η_j|<1
pp √s= 7 TeV, 1 < dN_ch/dη / ⟨ dN_ch/dη ⟩ < 2, |η_j|<1
pp √s= 7 TeV, 2 < dN_ch/dη / ⟨ dN_ch/dη ⟩ < 3, |η_j|<1
pp √s= 7 TeV, 3 < dN_ch/dη / ⟨ dN_ch/dη ⟩ < 4, |η_j|<1
pp √s= 7 TeV, 4 < dN_ch/dη / ⟨ dN_ch/dη ⟩ < 5, |η_j|<1
pp √s= 7 TeV, 5 < dN_ch/dη / ⟨ dN_ch/dη ⟩ < 6, |η_j|<1
pp √s= 7 TeV, 6 < dN_ch/dη / ⟨ dN_ch/dη ⟩ < 7, |η_j|<1
pp √s= 7 TeV, 7 < dN_ch/dη / ⟨ dN_ch/dη ⟩ < 8, |η_j|<1
pp √s= 7 TeV, 8 < dN_ch/dη / ⟨ dN_ch/dη ⟩ < 9, |η_j|<1
Pythia 8.180
number of jets (charged constituents)

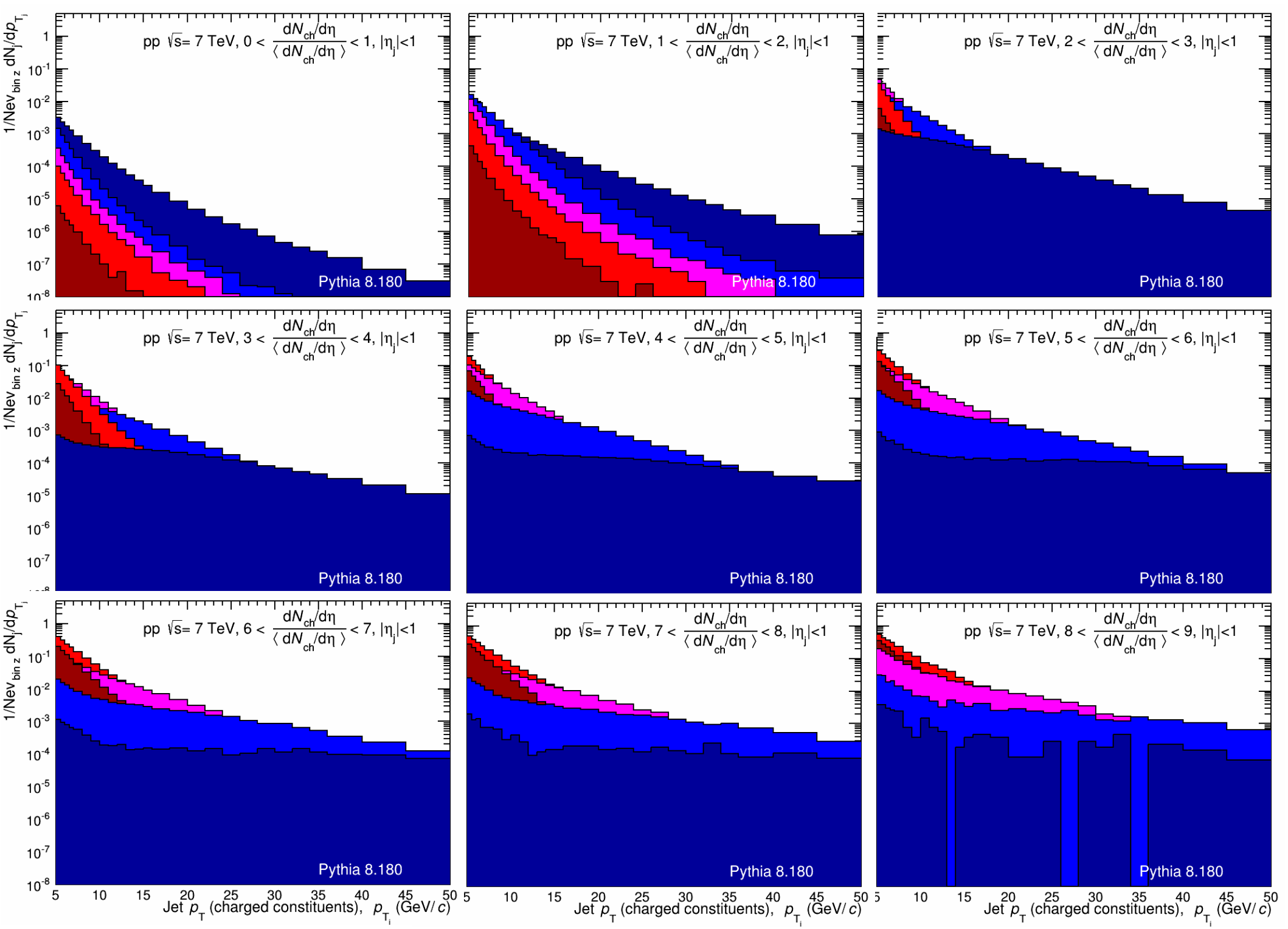
pp √s= 7 TeV, 0 < dN_ch/dη / ⟨ dN_ch/dη ⟩ < 1, |η_j|<1
pp √s= 7 TeV, 1 < dN_ch/dη / ⟨ dN_ch/dη ⟩ < 2, |η_j|<1
pp √s= 7 TeV, 2 < dN_ch/dη / ⟨ dN_ch/dη ⟩ < 3, |η_j|<1
pp √s= 7 TeV, 3 < dN_ch/dη / ⟨ dN_ch/dη ⟩ < 4, |η_j|<1
pp √s= 7 TeV, 4 < dN_ch/dη / ⟨ dN_ch/dη ⟩ < 5, |η_j|<1
pp √s= 7 TeV, 5 < dN_ch/dη / ⟨ dN_ch/dη ⟩ < 6, |η_j|<1
pp √s= 7 TeV, 6 < dN_ch/dη / ⟨ dN_ch/dη ⟩ < 7, |η_j|<1
pp √s= 7 TeV, 7 < dN_ch/dη / ⟨ dN_ch/dη ⟩ < 8, |η_j|<1
pp √s= 7 TeV, 8 < dN_ch/dη / ⟨ dN_ch/dη ⟩ < 9, |η_j|<1
Pythia 8.180
1/Nev_bin z dN_j/dp_Tj
Jet p_T (charged constituents), p_Ti (GeV/c)

Jet production vs N_{ch}

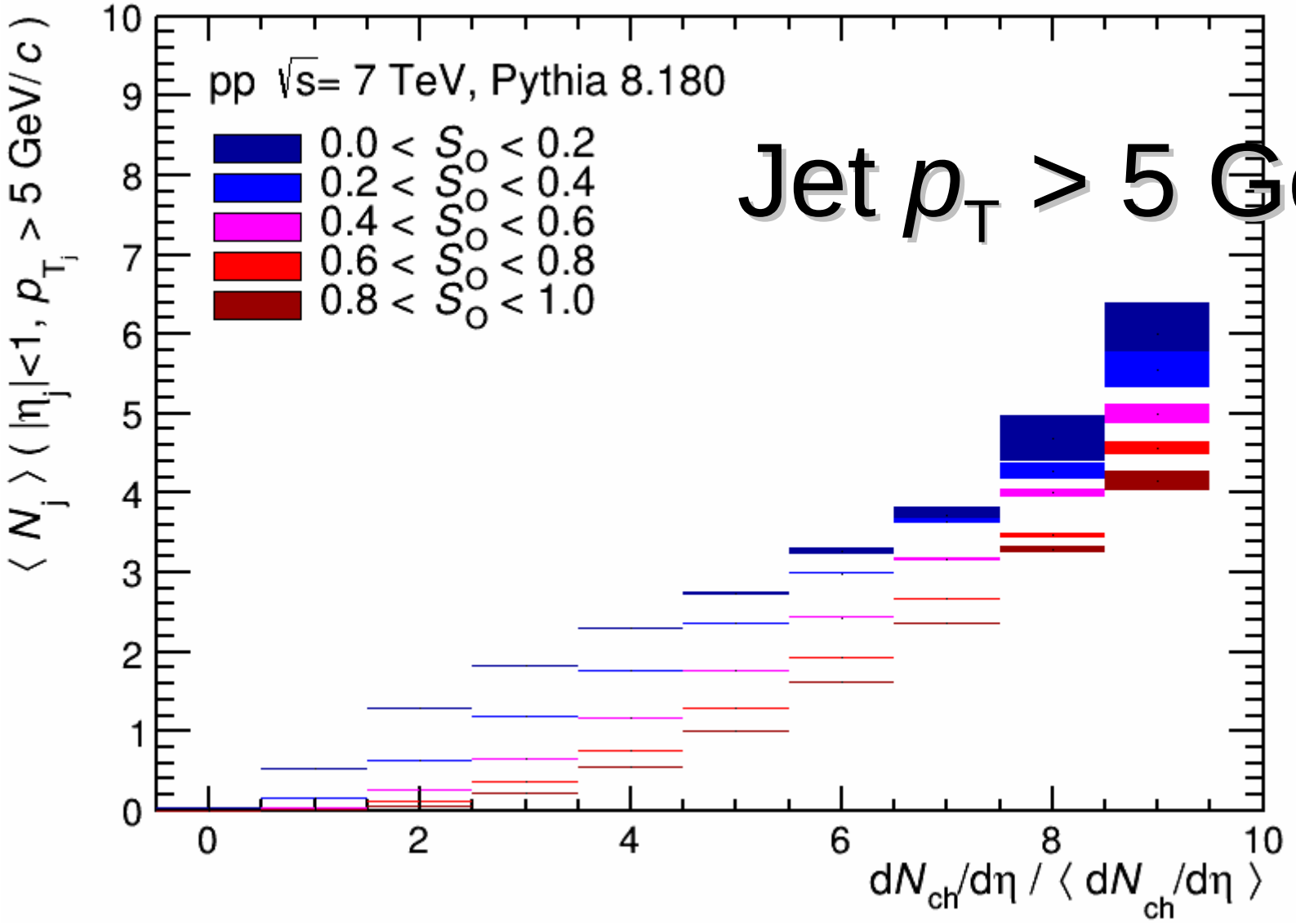

Jet production vs N_{ch}

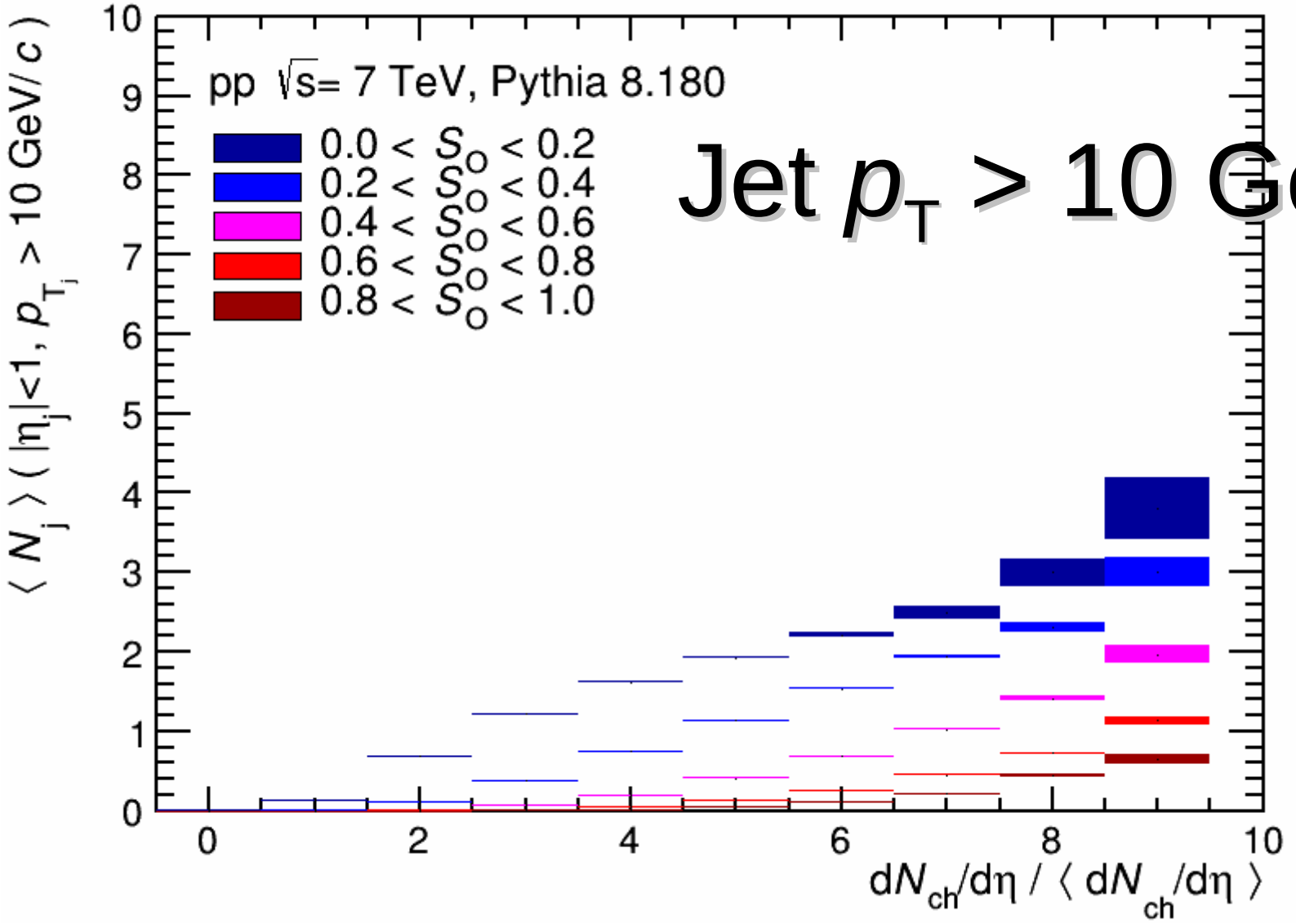

Jet p_T > 10 GeV/c

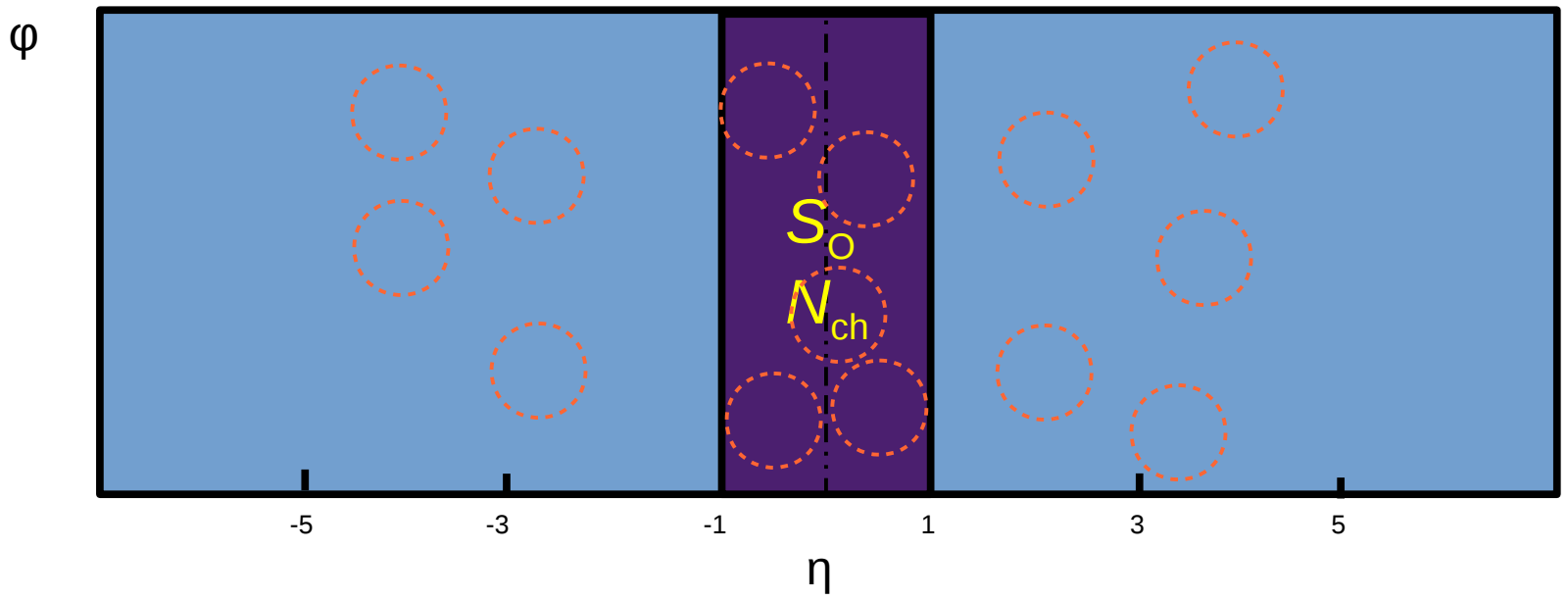

The next slides show the results where multiplicity and spherocity are calculated at mid-pseudorapidity interval (|η|<1). The jet finder is implemented in a wider pseudorapidity interval (|η|<5).

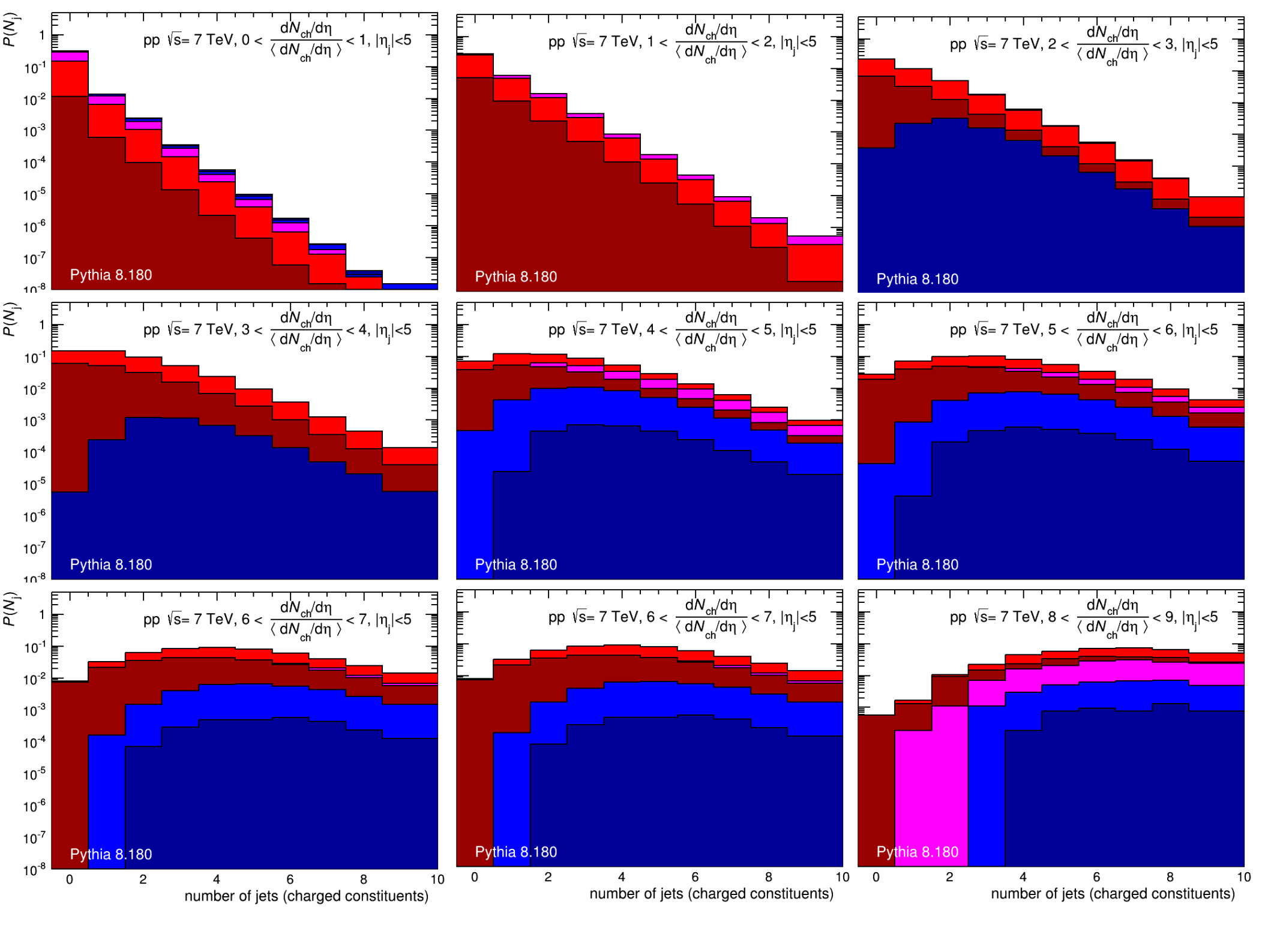
pp √s= 7 TeV, 0 < dN_ch/dη / ⟨ dN_ch/dη ⟩ < 1, |η_j|<5
pp √s= 7 TeV, 1 < dN_ch/dη / ⟨ dN_ch/dη ⟩ < 2, |η_j|<5
pp √s= 7 TeV, 2 < dN_ch/dη / ⟨ dN_ch/dη ⟩ < 3, |η_j|<5
pp √s= 7 TeV, 3 < dN_ch/dη / ⟨ dN_ch/dη ⟩ < 4, |η_j|<5
pp √s= 7 TeV, 4 < dN_ch/dη / ⟨ dN_ch/dη ⟩ < 5, |η_j|<5
pp √s= 7 TeV, 5 < dN_ch/dη / ⟨ dN_ch/dη ⟩ < 6, |η_j|<5
pp √s= 7 TeV, 6 < dN_ch/dη / ⟨ dN_ch/dη ⟩ < 7, |η_j|<5
pp √s= 7 TeV, 6 < dN_ch/dη / ⟨ dN_ch/dη ⟩ < 7, |η_j|<5
pp √s= 7 TeV, 8 < dN_ch/dη / ⟨ dN_ch/dη ⟩ < 9, |η_j|<5
Pythia 8.180
P(N_j)
number of jets (charged constituents)

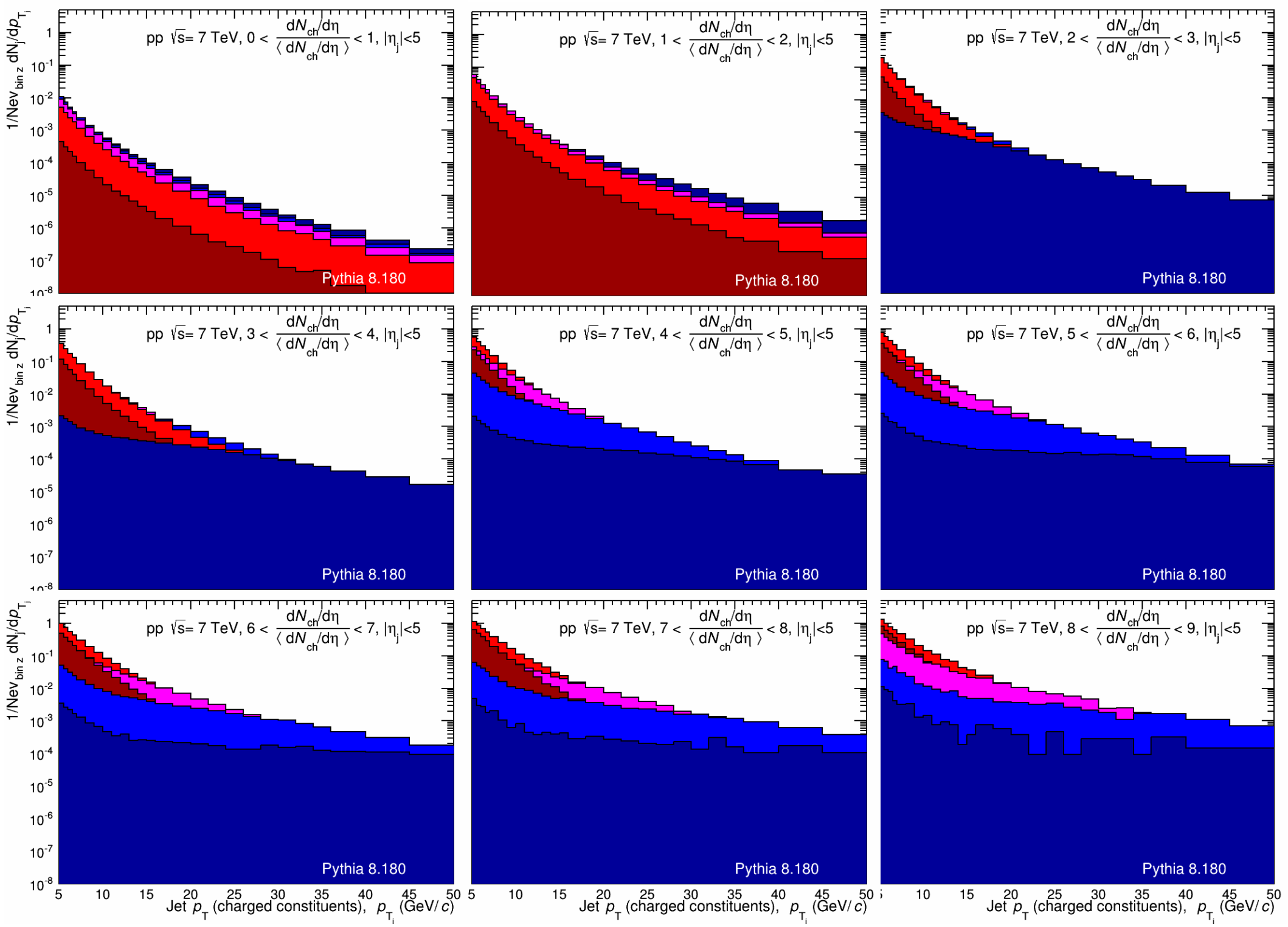
pp √s= 7 TeV, 0 < dN_ch/dη / ⟨dN_ch/dη⟩ < 1, |η_j|<5
pp √s= 7 TeV, 1 < dN_ch/dη / ⟨dN_ch/dη⟩ < 2, |η_j|<5
pp √s= 7 TeV, 2 < dN_ch/dη / ⟨dN_ch/dη⟩ < 3, |η_j|<5
pp √s= 7 TeV, 3 < dN_ch/dη / ⟨dN_ch/dη⟩ < 4, |η_j|<5
pp √s= 7 TeV, 4 < dN_ch/dη / ⟨dN_ch/dη⟩ < 5, |η_j|<5
pp √s= 7 TeV, 5 < dN_ch/dη / ⟨dN_ch/dη⟩ < 6, |η_j|<5
pp √s= 7 TeV, 6 < dN_ch/dη / ⟨dN_ch/dη⟩ < 7, |η_j|<5
pp √s= 7 TeV, 7 < dN_ch/dη / ⟨dN_ch/dη⟩ < 8, |η_j|<5
pp √s= 7 TeV, 8 < dN_ch/dη / ⟨dN_ch/dη⟩ < 9, |η_j|<5
Pythia 8.180
1/Nev_bin z dN_j/dp_T_j
Jet p_T (charged constituents), p_T_j (GeV/c)

Averages vs N_{ch}

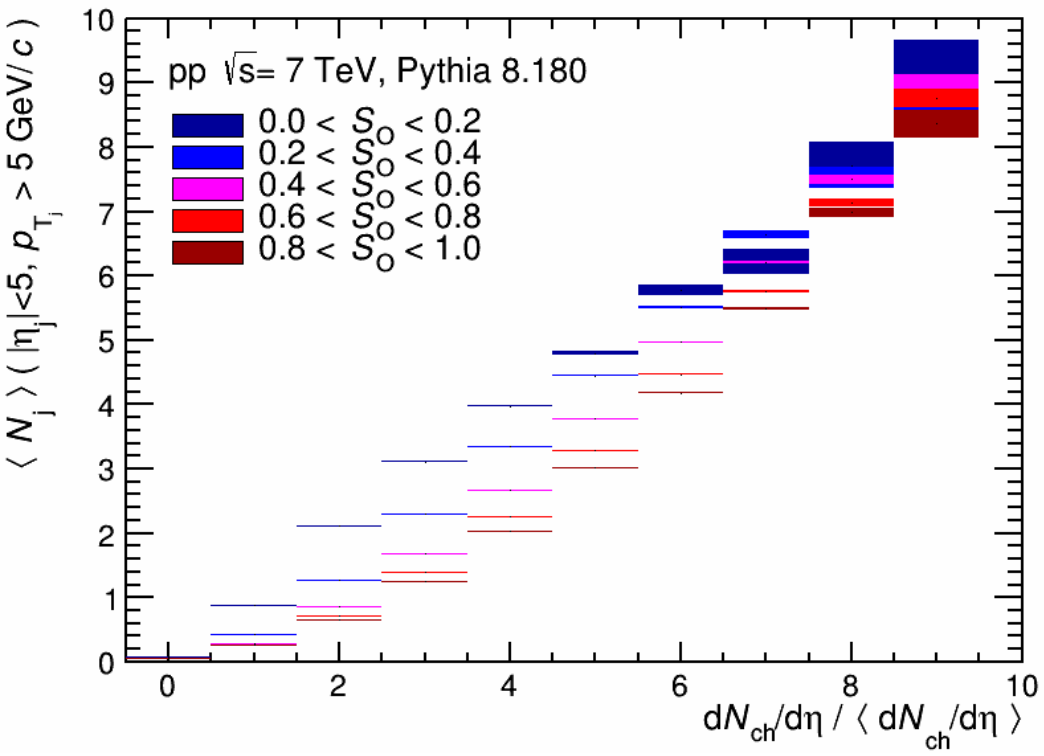

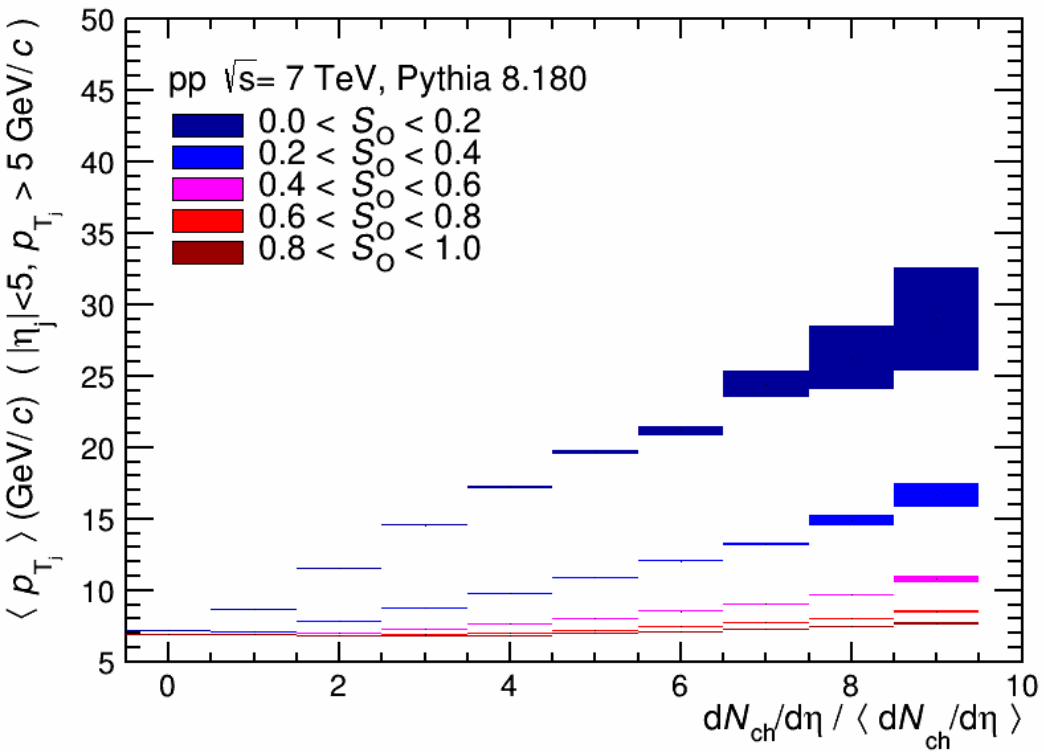

S_O including neutral hadrons

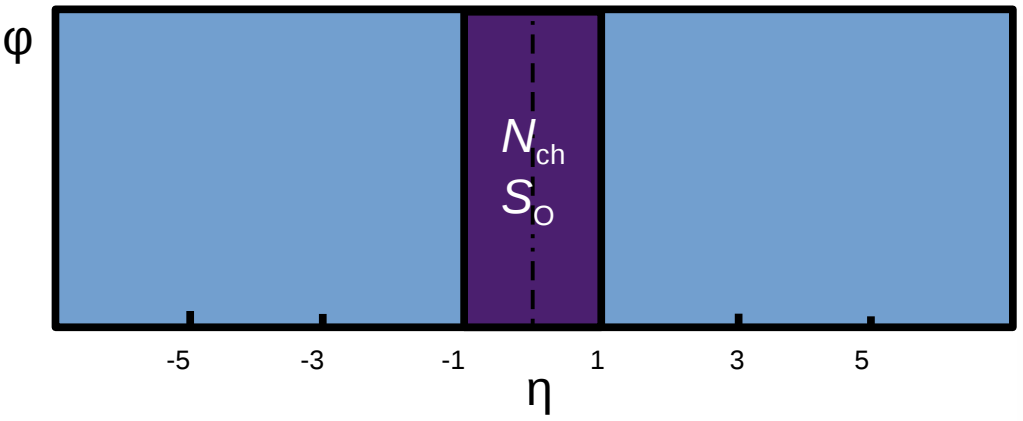

Correlation between transverse spherocity obtained using only charged hadrons vs the one including neutral hadrons.

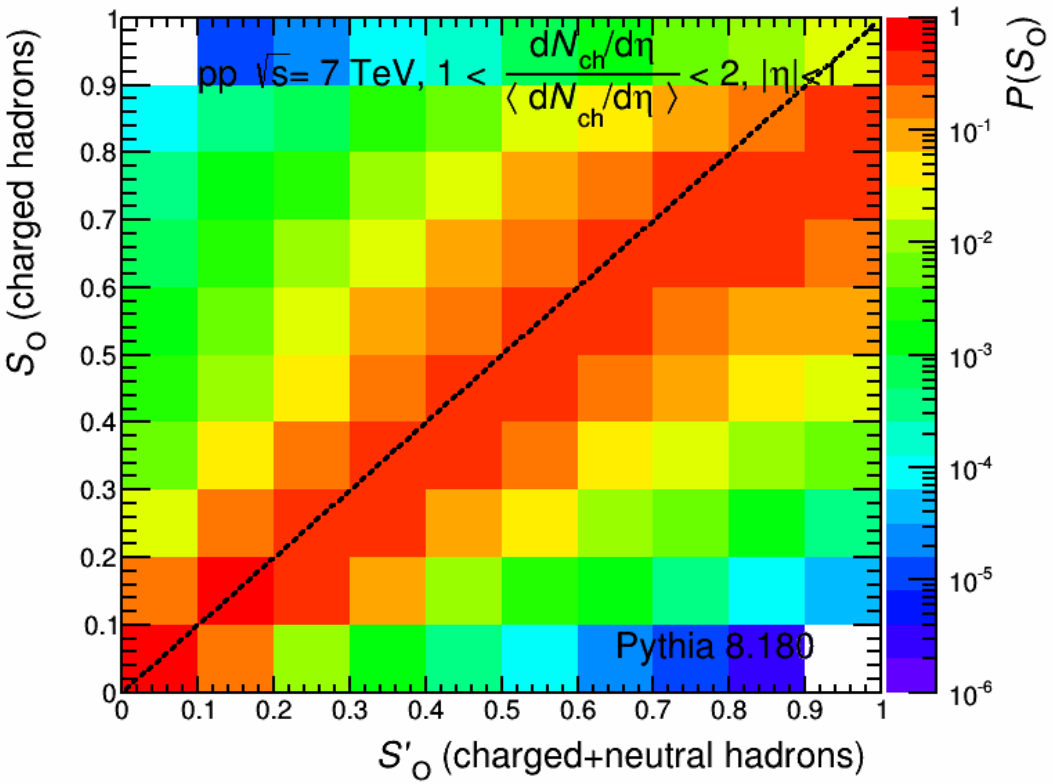

Result for Low mid-rapidity charged hadron multiplicity. The distribution becomes narrower with increasing multiplicity.

S_O including neutral hadrons

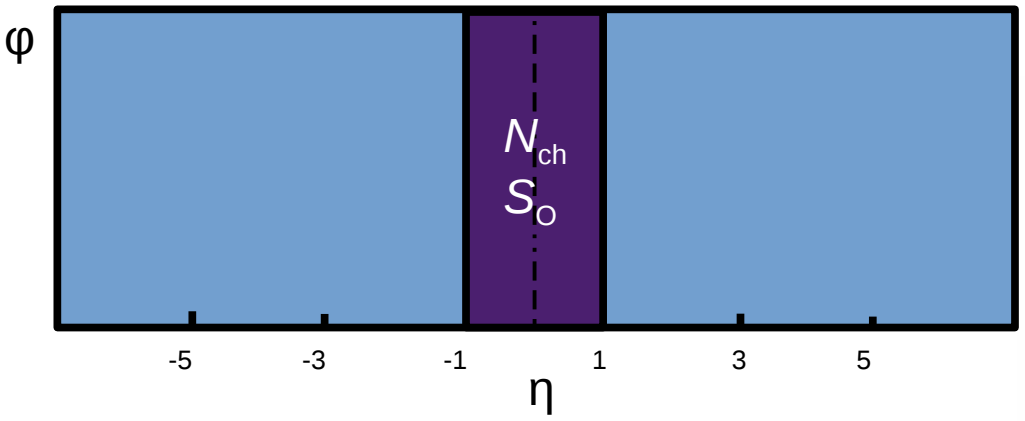

Correlation between transverse spherocity obtained using only charged hadrons vs the one including neutral hadrons.

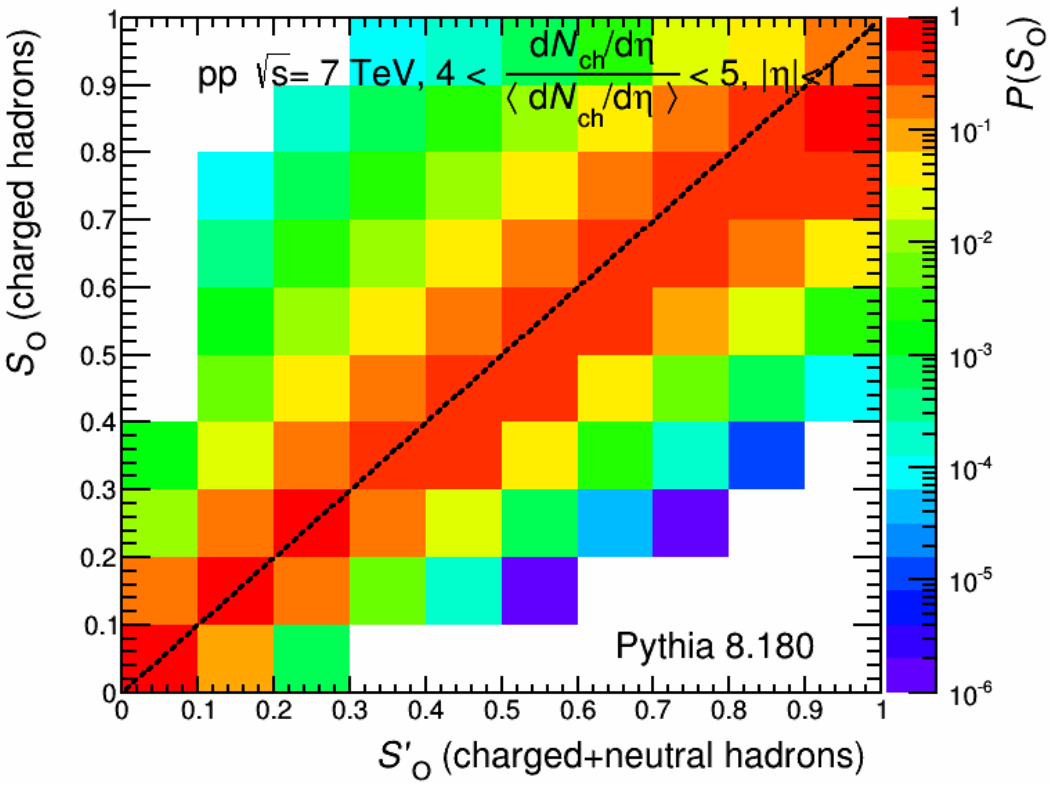

High mid-rapidity charged hadron multiplicity